Global and Planetary Change 259 (2026) 105351

Contents lists available at ScienceDirect

Global and Planetary Change

journal homepage: www.elsevier.com/locate/gloplacha

Research Article

Basement highs and their influence on basin geometry and sediment distribution in the Chacopampean Plain, Argentina☆

Valentina Cortassa [a,b,*], Stefan Back [c,d], Robert Ondrak [e], Cecilia del Papa [f], Eduardo Rossello [b], Manfred R. Strecker [a]

[a] Institute of Geosciences, University of Potsdam, 14476 Potsdam, Germany
[b] Instituto de Geociencias Básicas, Aplicadas y Ambientales, Universidad de Buenos Aires, 1428 Buenos Aires, Argentina
[c] Geological Institute, RWTH Aachen University, Wüllnerstr. 2, 52062 Aachen, Germany
[d] Tectonics and Geodynamics, RWTH Aachen University, Lochnerstr. 4–20, 52056 Aachen, Germany
[e] Organic Geochemistry Section, GFZ German Research Center for Geosciences, Telegrafenberg, 14473 Potsdam, Germany
[f] Cicterra, CONICET-University of Córdoba, 5016 Córdoba, Argentina

ARTICLE INFO

Editor Name: Dr. Sun Jimin

Keywords:
Andean foreland
Seismic interpretation
Inherited structures
Basement highs
Chacoparaense basin
North Argentina

ABSTRACT

The Chacopampean Plain of the Andean foreland of northern Argentina hosts an important sedimentary record that spans from the Paleozoic era to the present day. This study focuses on the analysis of the structural and sedimentary evolution of three distinct phases of basin history: i) the development of the Paleozoic intracratonic Chacoparanaense Basin; ii) the formation of the Cretaceous Salta Rift Basin; and iii) the Cenozoic formation of the Andean Foreland Basin. A comprehensive analysis of 3655 km of recently released industry seismic-reflection lines and stratigraphic information retrieved from 18 exploratory wells was conducted, enabling an unprecedented view of the complex tectonic and depositional history of the Chacoparanaense Basin. This history is closely associated with variable geodynamic boundary conditions that influenced this region until today. The Paleozoic and Mesozoic stages of basin evolution were finally superseded by deposition of an eastward-thinning sediment wedge of Andean Foreland Basin strata related to Cenozoic Andean mountain building, which began during the Paleogene.

The application of three-dimensional reconstruction techniques to the analysis of basin configurations through time has elucidated the significance of two prominent morphological structures in the subsurface, the Quirquincho and Pampeano-Chaqueño highs. These topographic highs exerted a long-lasting influence on sediment dispersal and deposition. Both basement highs were subsequently uplifted and partially eroded during the late Paleozoic and early Mesozoic, but progressively buried by sediments. The two elevated regions are interpreted as part of a Paleozoic forebulge that was formed by long-wavelength flexural uplift during the Gondwanan orogeny. The modification of these structures and the overlying sedimentary cover occurred during Cretaceous regional extension, a regional tectono-magmatic event that led to the formation of the Salta Rift Basin. The fact that Cenozoic foreland-basin deposits cover the paleo-topography of the Quirquincho and Pampeano-Chaqueño highs without notable interruption clearly shows that these sectors of the present-day foreland remained tectonically dormant during Cenozoic Andean shortening. This contrasts with adjacent areas of the foreland farther west that record structural overprinting during contractional inversion of Cretaceous extensional structures. The presented results highlight the intricate and non-linear impact of crustal memory on the evolution of foreland basins.

1. Introduction

The understanding of foreland basins straddling evolving mountain ranges is crucial in the context of paleo-environmental, paleo-climatic, and tectonic analyses at regional scales (DeCelles, 2011). More specifically, foreland basins contain valuable stratigraphic and lithologic information on the dynamic interplay between tectonic and climatic processes in the adjacent mountain ranges that may help to assess the

☆ This article is part of a Special issue entitled: 'sedimentary basins' published in Global and Planetary Change.

* Corresponding author at: Av. O'Higgins 5700, Barrio Greenville, Córdoba X5014, Argentina.
E-mail address: valentina.cortassa@gmail.com (V. Cortassa).

https://doi.org/10.1016/j.gloplacha.2026.105351
Received 22 May 2025; Received in revised form 24 January 2026; Accepted 29 January 2026
Available online 4 February 2026

effects of changing orogenic topography and relief on sediment production through time. In addition, these sediments may also provide insights regarding the history of tectonically-forced climate and surface-process conditions in the neighboring mountain ranges (Molnar et al., 1993; Grujic et al., 2006; Bookhagen and Strecker, 2008). Over time, foreland basins subside due to tectono-sedimentary loading, creating large accommodation space for sediments (DeCelles, 2011). Foreland basins are of direct economic relevance as they represent important hydrocarbon provinces (in South America, e.g., the Llanos Basin: Campos and Mann, 2015, Garcia Bautista et al., 2015; the Maracaibo Basin: Stauffer and Croft, 1995, Escalona and Mann, 2006, Mann et al., 2006; the Magdalena Valley Basin: Sarmiento and Rangel, 2004, Spickert, 2014; the Neuquén Basin: Howell et al., 2005, Veiga et al., 2020). Foreland basins may also contain geothermal energy plays, with the North Alpine Foreland Basin of Europe being a prime example of an economically important hydrothermal reservoir system (e.g., Obermeier et al., 2025).

Many studies of foreland basins have documented a direct linkage between orogenic loading and a flexural response, with a large negative flexure close to the load (foredeep), a central positive flexure (forebulge), and a small secondary negative flexure (backbulge) in distal regions (summarized in DeCelles, 2011). Yet, the flexural profile of a foreland basin depends on whether the orogenic load is supported by a continuous, elastic plate (Flemings and Jordan, 1989; Turcotte and Schubert, 2014); or a plate characterized by lithospheric heterogeneity (e.g., Sinclair et al., 1991; Blisniuk et al., 1998; Cloetingh et al., 2004). For example, pre-existing, inherited basement structures can be reactivated during crustal flexure (e.g., Crampton and Allen, 1995; Gupta and Allen, 2000), potentially influencing drainage development and, consequently, foreland-basin depositional patterns and stratigraphy (Horton and DeCelles, 1997; Hilley et al., 2005; Strecker et al., 2011).

This study focuses on the geological analysis of seismic-reflection and borehole data of the Chacopampean Plain of the Andean retroarc-foreland basin of northern Argentina (Figs. 1 and 2). Key study targets are two deeply buried, SW-NE-oriented basement ridges at the base of the modern foreland basin, the Quirquincho and Pampeano-Chaqueño highs (Fig. 3; Russo et al., 1979). The Quirquincho High is >400 km long and >100 km wide; the Pampeano-Chaqueño High is >150 km long and around 50 km wide (Fig. 3). Despite their large areal extent and prominent subsurface position, there are open questions regarding the origin of the basement structures, their evolution, and their potential influence on the development of the modern Andean foreland. Information on these topics is relevant for research on foreland-basin evolution in other regions, because the regional subsurface analyses presented here are among very few studies that document the role of subsurface topography and inherited structures in the subsurface of young foreland basins (e.g., Billi and Salvini, 2003; Roddaz et al., 2005; Reis et al., 2017);

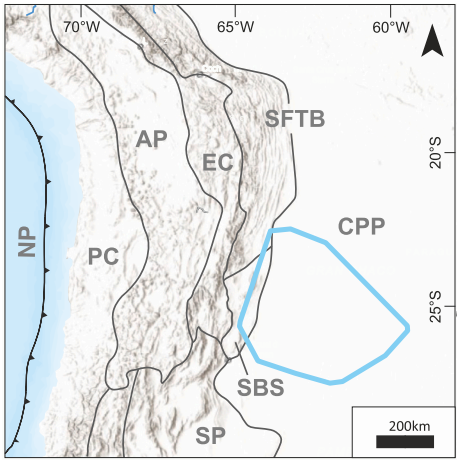

Fig. 1. Location of the study area and regional setting. Shaded relief map and principal morphotectonic provinces of the southern Central Andes (after Jordan *et al.*, 1983). Nazca plate, NP; Chacopampean Plain, CPP; Santa Barbara System, SBS; Andean Plateau, AP; Sierras Pampeanas, SP; Eastern Cordillera, EC; Subandean foreland fold-and-thrust, SFTB; Principal Cordillera, PC. The study area is outlined by the blue polygon.

2. Geological setting

2.1. Chacopampean Plain

The Chacopampean Plain in the Andean foreland of northern Argentina is a lowland close to sea level in the east and reaches up to 500 m elevation near the Andes in the west. It is covered by a thin (~50 m in places, Torre et al., 2025), continuous Quaternary deposit of loess, fluvial, and lacustrine strata (Fig. 2; Russo et al., 1979). The Chacopampean Plain has received sediments from the uplifting Andes since the middle Eocene (Carrapa et al., 2012; del Papa et al., 2013). At present, the region is characterized by either transient sediment storage or the transfer of sediments from the Andean orogen to the Atlantic Ocean, with limited subsidence and a low sedimentation rate (Russo et al., 1979; Chebli et al., 1999; Repasch et al., 2021, 2023). Beneath the Quaternary foreland-basin deposits lie older sediments (Fig. 4) that are associated with several depocenters of different locations and geological age that are separated by two structures: the Quirquincho and Pampeano-Chaqueño highs (Fig. 2; Russo et al., 1979; Chebli et al., 1999; Cortassa et al., 2022). Chronologically, the oldest part of the Chacopampean subsurface constitutes the Chacoparanaense Basin of Paleozoic sediments, succeeded by the strata of the extensional Salta Basin, and finally the deposits of the Andean Foreland Basin.

2.2. Chacoparanaense Basin

The Chacoparanaense Basin is a >1,000,000 km^2 (Chebli et al., 1999) NNE-trending Paleozoic basin that extends from northern Argentina northward into Paraguay and Brazil (Fig. 2). It likely originated from Proterozoic rifting and developed throughout the Paleozoic and Mesozoic by thermal subsidence at the southwestern margin of Gondwana (Russo et al., 1979; Chebli et al., 1999; Reinante et al., 2014). The basin is characterized by a faulted basement with several depocenters bordered by highs, interpreted as having formed either during the Paleozoic Pampean and Gondwanic orogenies, potentially in the context of Mesozoic rift-shoulder uplift (e.g., Fernández Garrasino et al., 2005) or during Cenozoic basin inversion driven by Andean shortening (e.g., Chebli et al., 1999; Ramos et al., 2006).

Four boreholes penetrate the Precambrian crystalline (diorite 2162 ± 6 Ma; and granite, 2088 ± 6 Ma) and metasedimentary (amphibolitic schist, 2189 ± 14 Ma) basement of the Chacoparanaense Basin (Rapela et al., 2007; Favetto et al., 2015), which is unconformably overlain by Paleozoic and younger strata (Fig. 4; Russo et al., 1979; Chebli et al., 1999; Fernández Garrasino et al., 2005). The Paleozoic strata comprise three dominantly marine sedimentary intervals of Cambrian-Ordovician, Silurian-Devonian, and Carboniferous-Permian ages, all separated by distinct angular unconformities (Fig. 4; Russo et al., 1979). The Cambrian-Ordovician clastic basin fill was deposited in a marine shelf environment (Russo et al., 1979; Chebli et al., 1999; Fernández Garrasino et al., 2005). Silurian-Devonian sediments include the Zapla Formation diamictite, which gradually transitions into dark grey, pyritic, laminated shale likely deposited in a calm, relatively deep marine environment (Fig. 4; Russo et al., 1979). This unit is overlain by fine, whitish grey quartzitic sandstone and black shale. The Carboniferous-Permian sedimentary record comprises sandstones overlain by black shale (Russo et al., 1979), probably deposited in a glacio-lacustrine environment (Fernández Garrasino et al., 2005).

The Mesozoic units of the Chacoparanaense Basin (Fig. 4) are mostly clastic sediments of continental origin (Fernández Garrasino et al., 2005). The sediments in the Argentine part of the basin (Fig. 3) are

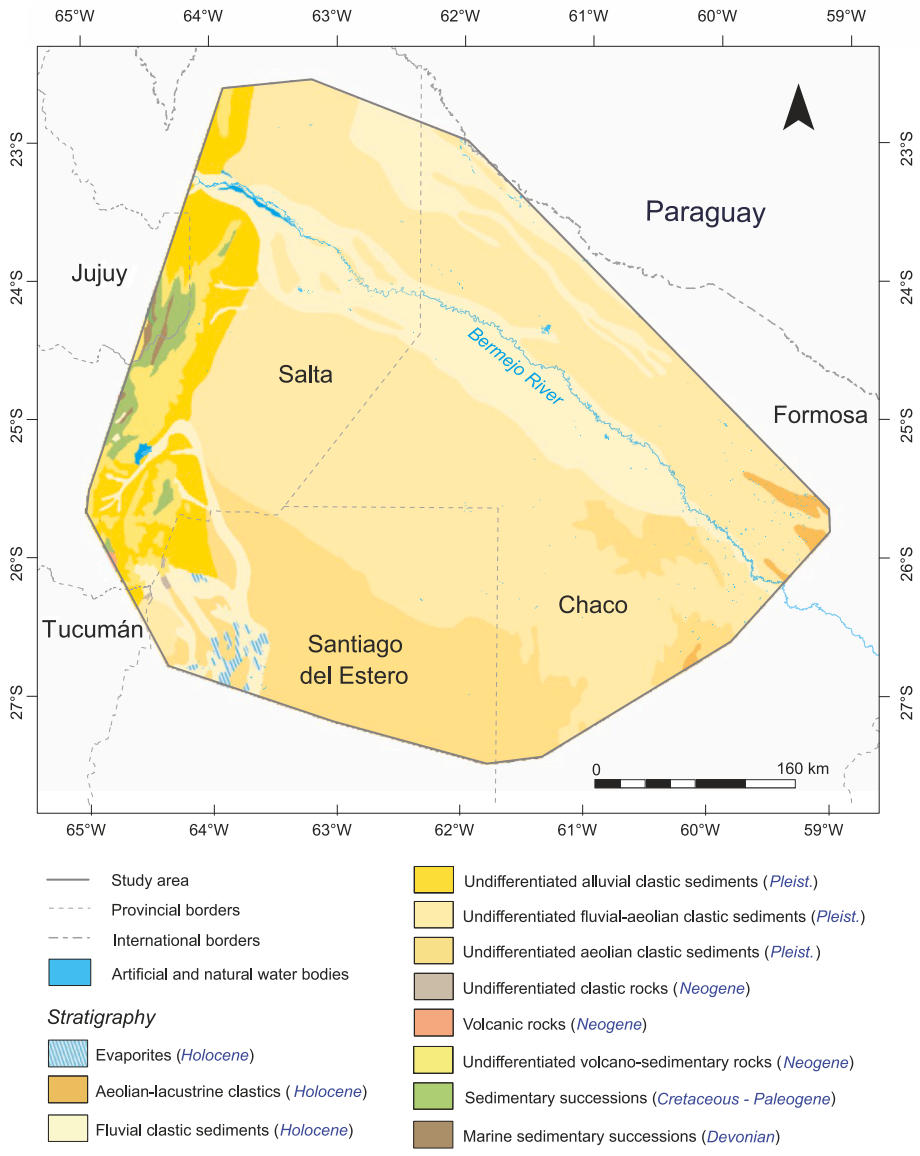

Fig. 2. Geological map of the study area (Modified from IGN Argentina - www.ign.gob.ar).

predominantly of Cretaceous age, although Triassic or Jurassic sediments might occur. Age control is poor due to the scarcity of fossils in drill cuttings (Chebli et al., 1999). Overlying Cenozoic strata are terrestrial clastic rocks (Fig. 4) except for a series of shale and sandstones that record a major transgression in the middle Miocene (Russo et al., 1979). The Miocene Paranaense Sea covered almost the entire basin and reached the location of the present-day eastern Andean Cordillera (Fig. 1; Russo et al., 1979; Ramos and Alonso, 1995; Chebli et al., 1999).

2.3. Salta Rift Basin

The Salta Rift evolved on heterogeneous basement rocks that span from the Precambrian to the Jurassic, including various sedimentary units belonging to the Tarija Basin in Bolivia (Fig. 3; e.g., Cediel et al., 2003). The Salta Rift Basin was magmatically active in the Cretaceous, during the opening of the Atlantic Ocean (Starck, 2011). The basin has three subbasins or main depocenters, including the Tres Cruces depocenter in the NW, the Metán-Alemanía depocenter in the S, and the Lomas de Olmedo depocenter in the E (Fig. 3). This study covers the Lomas de Olmedo and eastern Metán-Alemanía depocenters, in which the Cretaceous-Paleogene Salta Group (Turner, 1959) was deposited. The Salta Group can be divided into three subgroups: the Pirgua Subgroup (Reyes and Salfity, 1973), which comprises clastics and volcanic rocks formed during the *syn*-rift stage; and the late Cretaceous Balbuena and Santa Bárbara subgroups that contain both clastic sediments and carbonates (Moreno, 1973) deposited during thermal subsidence stage (Fig. 4). The Salta Group rocks are exposed in the Subandean thin-skinned fold-and-thrust belt to the northwest, the Eastern Cordillera, the northern Sierras Pampeanas, and the Andean Puna Plateau (Fig. 1) (Salfity and Marquillas, 1994).

Salta Rift Basin extension was from 82 to 75 Ma (Gallinski & Viramonte, 1988; Starck, 2011) followed by thermal subsidence (e.g., Marquillas et al., 2005; Ruiz-Monroy, 2021; Mutti et al., 2023; Vallati et al., 2023). Subsequent Andean shortening (Cobbold et al., 2007; Starck, 2011) inverted parts of the Salta Rift (Jordan et al., 1983; Coutand et al., 2001; Kley and Monaldi, 2002; Oncken et al., 2006; Carrera and Muñoz, 2008; Hain et al., 2011; Arnous, 2021; Arnous et al., 2024) by contractionally reactivating former extensional structures (Grier et al., 1991; Allmendinger et al., 1997; Kley and Monaldi, 2002; Carrapa et al., 2005; Carrera et al., 2006; Kley et al., 2005; Iaffa et al., 2011; Arnous et al., 2024).

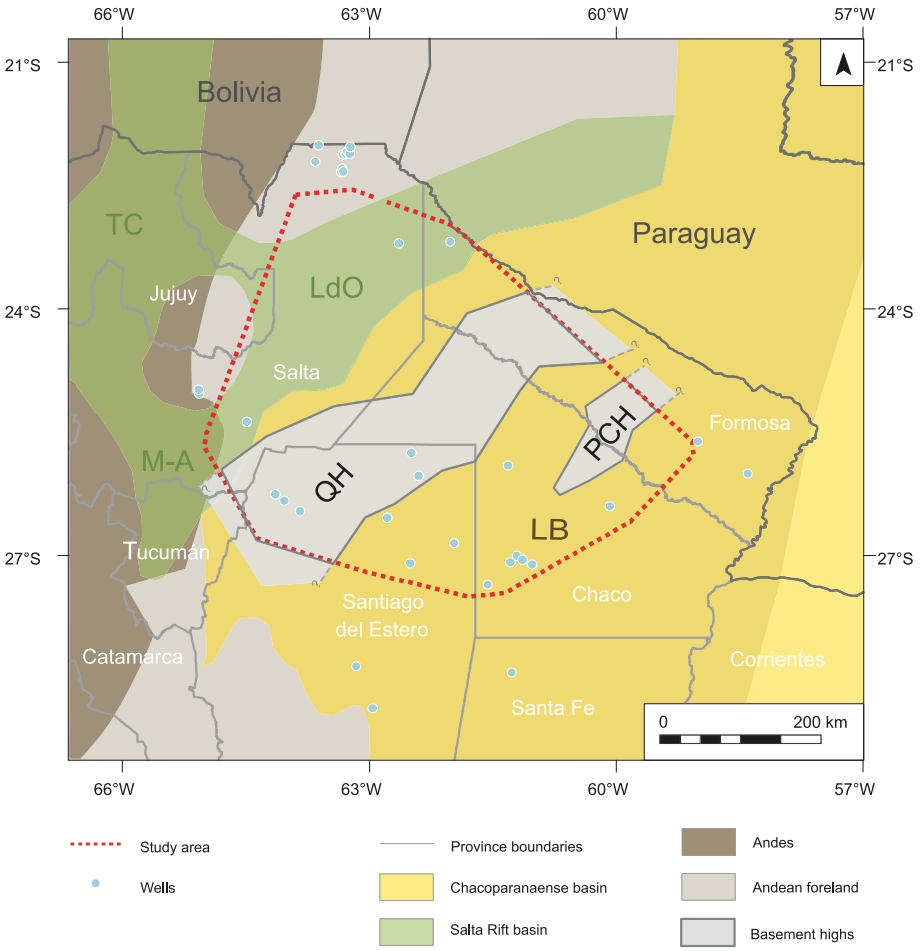

Fig. 3. Provincal and political boundaries in the Chacopampean Plain with outlined underlying basin systems and depocenters. Tres Cruces depocenter, TC; Lomas de Olmedo depocenter, LdO; Metán-Alemanía depocenter, M-A; Las Breñas depocenter, LB; Quinquincho High, QH; Pampeano-Chaqueño High, PCH.

3. Data and methods

We analyzed 95 2D seismic profiles with a total length of 3650 km, and information from 18 petroleum exploration wells (Fig. 5, Cortassa et al., 2025). Access to subsurface data (2D seismic lines and well logs) as paper copy and/or scanned image was kindly provided by BHP Petroleum Argentina (S.A.). The 2D seismic-reflection data in the study area were acquired by different companies between 1943 and 1990. Seismic sources were either dynamite or vibroseis. In most cases the receiver spacing was 50 m, in a few surveys 25 m or 100 m. Typical recording frequencies were between 12 and 15 and 60 Hz, and the respective recording lengths were 4, 5 or 6 s. The seismic-reflection lines are of variable quality, ranging from poor to medium in terms of identifiable reflectors and reflection patterns.

In order to allow digital seismic interpretation in three dimensions, we converted scans of the seismic data into SEG-Y format using the free software Kogeo Seismic Toolkit. We then georeferenced all seismic profiles (including mis-tie management and topographic balancing), and interpreted them using Kingdom Suite 2016 and Petrel softwares.

The borehole information for this study (in total 18 wells) includes coordinates, well tops, lithology, and sonic surveys from borehole reports from Pirané (Rolleri, 1965) and Chirete (Pluspetrol, 1990) along for the Northern Transect (Figs. 5, 6); and Las Breñas 1 (Bottcher, 1974), Las Breñas 2 (Rolleri, 1967), Las Breñas Oriental (Rolleri, 1966), Coronel Rico (Di Persia, 1969), El Caburé (Bottcher, 1965), Los Horcones 1 (Di Persia, 1970), Los Horcones 2 (Moreno, 1973), and Cerro Colorado (Pluspetrol, 1990), for the Southern Transect (Figs. 5, 7).

3.1. Seismic interpretation and horizon flattening

We used well data to tie the seismic interpretations to the units described in the wells and to identify the reflectors corresponding to unit tops. We tracked marker horizons across the study area and marked unconformities indicated by onlaps and reflection truncations.

By combining several seismic profiles and their interpreted horizons, we constructed the Northern Transect (NT) with a length of 750 km and the Southern Transect (ST) with a length of 500 km (Figs. 6, 7). Both transects are approximately NW–SE–oriented. The Northern Transect (Fig. 6) has better lateral continuity and is composed of nine individual 2D seismic reflection surveys. The Southern Transect (Fig. 7) comprises four 2D seismic surveys plus a portion of one N-S-oriented survey. The Southern Transect has less lateral continuity, which we compensated for by extrapolation of interpreted seismic segments, well information, and horizon interpolation. We divided the sedimentary fill of the Chacoparanaense Basin, the Cretaceous Salta Rift, and the Cenozoic Andean Foreland Basin into five marker horizons and five principal seismic reflection units. From base to top (old to young), the marker horizons are H1 (Top Precambrian), H2 (Top Paleozoic), H3 (Top Cretaceous), H4 (Top Paleogene), and H5 (Top Neogene). The present-day topography is the upper boundary of the interpreted sedimentary succession. Above the acoustic basement, the horizons bound the seismic reflection units labeled U1 to U5 (from old to young). Formation tops determined in boreholes defined horizons and unit ages, while all horizons follow (relatively) continuous seismic reflectors. To better understand the stratal terminations and the relationship between succeeding geological units, we used horizon flattening (Fig. 8).

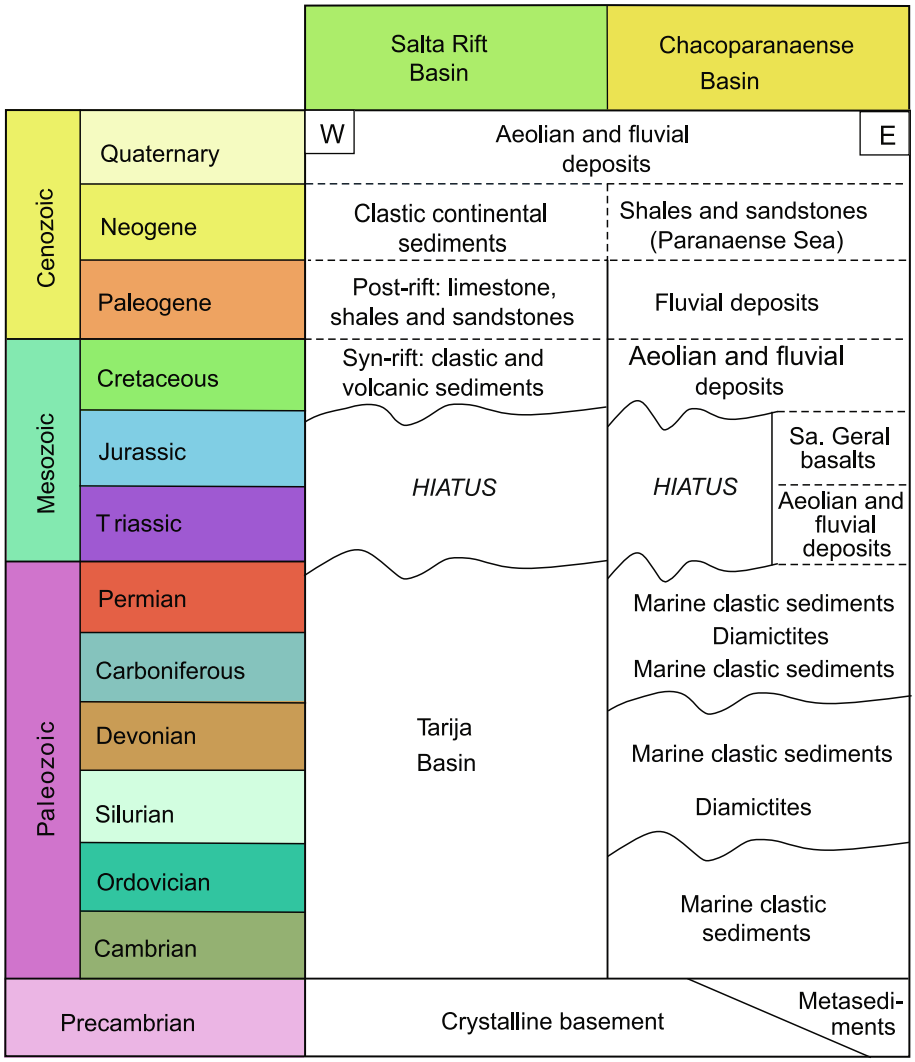

Fig. 4. Stratigraphic columns of the Salta Rift and Chacoparanaense basins (Russo *et al.*,1979) based on well reports (e.g., Rolleri, 1965; Rolleri, 1966; Rolleri, 1967; Bottcher, 1965; Bottcher, 1974; Di Persia, 1969; Di Persia, 1970; Moreno, 1973; Pluspetrol, 1990; Pluspetrol, 1995), Starck, 2011 and Marquillas *et al.* 2005.

3.2. Velocity models for time-depth conversion

To correlate well-formation tops with seismic horizons, we produced velocity models. We analyzed and compiled data from the headers of 19 seismic profiles of the Salta Rift Basin and nine seismic profiles of the Chacoparanaense Basin. This data was the equivalence between two-way travel time (TWT) in milliseconds and depth (Z) in meters, and it was plotted in X–Y charts with each point corresponding to a one-point value of the check shot. With this point cloud, we calculated trend lines of time-depth conversion rates (Fig. 9).

3.3. Depth and thickness maps

We imported all of the interpreted seismic lines and their depth-converted horizons into Petrel 2015 E&P Software (Schlumberger), interpolating between them to create depth and thickness maps. We constructed four depth maps (Fig. 10) for the top of the Precambrian basement (H1), the top of the Paleozoic sediments (H2), the top of the Cretaceous sediments (H3), and the top of the Paleogene sediments (H4). Subsequently, we calculated isopach maps (Fig. 11) for the Paleozoic Unit U1, the Cretaceous Unit U2, the Paleogene Unit U3, and the Neogene Unit U4.

4. Results

4.1. Seismic Interpretation

4.1.1. Horizon Interpretation

Seismic horizon H1 is the deepest horizon identified; it can be recognized in numerous sectors of the study area. H1 defines the boundary between chaotic, disrupted low-to-medium amplitude reflections and the overlying semi-continuous to continuous reflections with subparallel, parallel, and in places divergent reflection patterns. H1 follows a high-amplitude positive reflection and is observed at different depths, being much deeper in the west. H1 is intersected by a normal fault in the area of the Pampeano-Chaqueño High in the Northern Transect (Fig. 6) and by a normal fault bounding the Las Breñas half-graben in the Southern Transect (Fig. 7). In the Southern Transect (Fig. 7), a local H0 horizon (inferred) is included, separating acoustic units in the basement of the Las Breñas half-graben of sedimentary Precambrian rocks at the top, from the underlying crystalline units (Chebli et al., 1999).

We mapped seismic horizon H2 on a high-amplitude reflector of variable continuity. H2 is much deeper in the west than in the east. Its morphology is irregular with a wavy to distorted character in the east and the center of the Southern Transect (Fig. 7), and generally west-dipping. Several faults cut H2 in the western part of the study area,

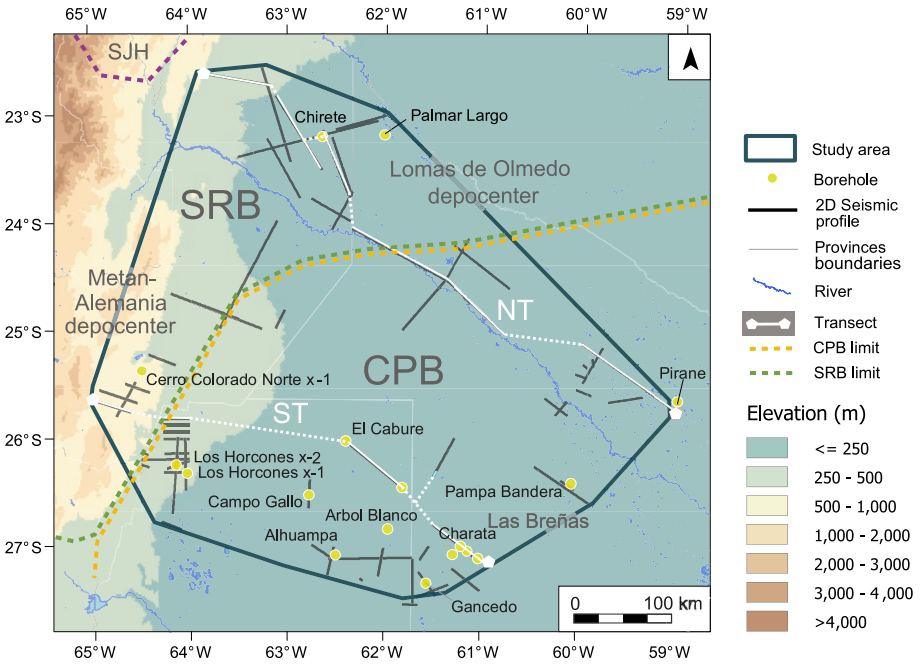

Fig. 5. Digital elevation model (from USGS Earth Explorer portal) and surface hydrographic conditions (IGN-Argentina database- www.ign.gob.ar) of the study area. Location of seismic profiles, wells, Northern (Northern Transect) and Southern (Southern Transect) seismic transects (continuous white lines indicate the location of the analyzed seismic profiles and the dotted lines denote the data gaps or interpolated areas.), including location of the Salta Rift (SRB) and Chacoparanaense Basins (CPB) with main depocenters.

with the most prominent normal faults defining a graben (Figs. 6, 7). To the east, in the Southern Transect (Fig. 7), H2 is displaced by a west-dipping normal fault near the Coronel Rico (CR) well and by a series of normal faults at the eastern end of the transect near the Las Breñas 2 (LB2) well.

Seismic horizon H3 is a reflector with high amplitude, flanked by two parallel, low-amplitude reflections. In the west of the study area (Fig. 6), H3 dips to the west and is cut by two faults delimiting a graben structure, about 100 km in width and 1000 ms (TWT) in depth. A normal fault is observed in the Southern Transect (Fig. 7), forming a depocenter with dimensions of approximately 50 km in width and 800 ms (TWT) in depth. H3 onlaps onto H2 at the Quirquincho High (Fig. 6) and is not present in the central part of the high. We interpret a similar onlap and distribution of the disappearance of H3 in the Southern Transect (Fig. 7). East of the Southern Transect, two paired normal faults cut H3 close to the Las Breñas 2 well.

The H4 seismic horizon is a laterally continuous reflector with high positive amplitude that varies greatly in depth. H4 onlaps the Pampeano-Chaqueño High and a large portion of the Quirquincho High (Northern Transect – Fig. 6). Seismic horizon H5 is a laterally continuous reflector with high amplitude, and which varies much less in depth than the position of older horizons. It is absent in most of the Southern Transect (Fig. 7).

4.1.2. *Unit Interpretation*

In the deepest (TWT) parts of profiles, the acoustic basement is characterized by chaotic, disrupted low-to-medium amplitude reflections. Seismostratigraphic unit U0 (correlative to late Precambrian metasediments; Fig. 7) is located at the eastern end of the Southern Transect between H0 at the base and H1 at the top. U0 has low-amplitude, low-frequency, and low-continuity reflections. This unit has a wedge shape bounded by a normal fault in the thickest area (west), whereas it thins and pinches out to the east.

Seismostratigraphic unit U1 (correlative to Paleozoic; Figs. 6, 7) is bounded by horizons H1 (base) and H2 (top). It has reflections of variable amplitude, medium frequency, and medium to low continuity. U1 shows an irregular sheet-like shape with some thicker areas. An example is the area beneath the Quirquincho High (Fig. 6), with a thickness of about 1100 ms (TWT) in the Northern Transect and 1600 ms (TWT) in the Southern Transect. Toward the west of the Quirquincho High, U1 attains a minimum thickness of ~300 ms (TWT) (Northern Transect, Fig. 6). U1 is laterally discontinuous due to two normal faults forming a graben corresponding to the Metán-Alemanía depocenter (Fig. 5) in the Southern Transect (Fig. 7).

Seismostratigraphic unit U2 (correlative to Cretaceous; Figs. 6, 7) is bounded by horizons H2 (base) and H3 (top). U2 has high-amplitude reflectors in the eastern and central parts of the study area that decrease in amplitude strength toward the Salta Rift Basin to the west (Figs. 6, 7). The reflections have medium frequency and medium lateral continuity. U2 displays a lens shape in its lower part between the Quirquincho and Pampeano-Chaqueño highs. It disappears in the central part of Quiquincho High while attaining a subtle wedge geometry in the west of this high, thickening toward the west. In the Salta province (Northern Transect, Fig. 6), U2 fills the graben (thickness ~ 1000 ms TWT) bounded by two normal faults (Lomas de Olmedo depocenter). Within this graben, the internal reflections of U2 are subparallel and locally folded.

Seismostratigraphic unit U3 (Figs. 6, 7) is bounded by horizons H3 (base) and H4 (top). It has medium to low-amplitude reflectors with medium to low frequency and medium lateral continuity. Its reflections are parallel in the east, subparallel in the central-western area, and locally folded within the graben structure (Fig. 6). As in the underlying unit U2, the Quirquincho and Pampeano-Chaqueño highs intersect U3. In the western and central parts of the study area, the unit has the shape of a large westward-thickening wedge with an irregular lower boundary due to the presence of faults. In the Metán-Alemanía graben, U3 reaches a maximum thickness of ~1700 ms (TWT). U3 significantly thins toward the Quirquincho and Pampeano-Chaqueño highs, and onlaps both structures (Northern Transect, Fig. 6). To the east of the Pampeano-Chaqueño High, U3 maintains a constant thickness of ~100 ms. At the eastern end of the Southern Transect (Fig. 7), normal faults cut U3 in its lower section at the location of the Las Breñas 2 (LB2) well. Between the

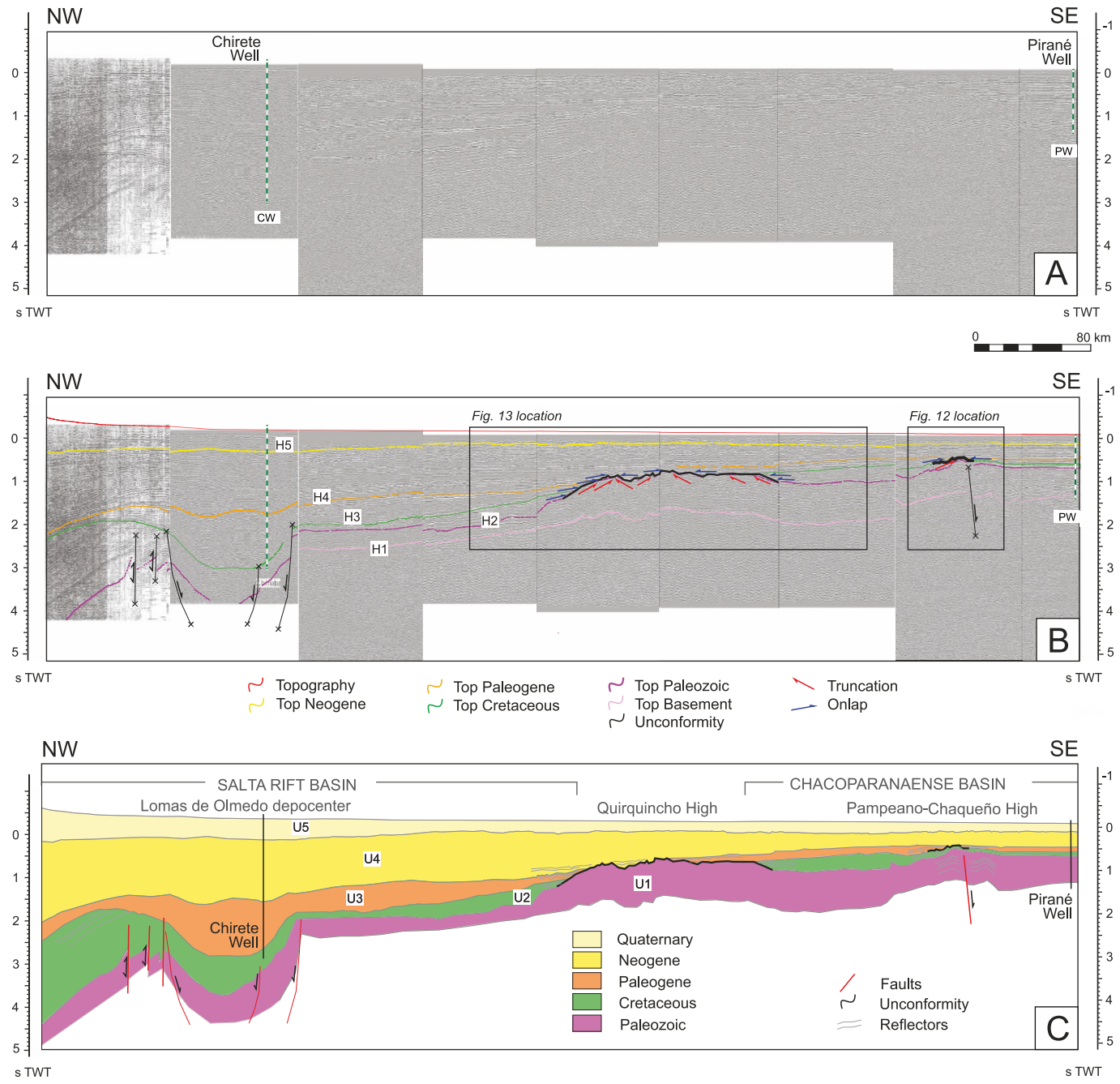

Fig. 6. NW-SE-oriented Northern transect (NT) (see Fig. 5 for location). A- Uninterpreted seismic lines. B- Seismic profiles with interpreted color-coded horizons (H1: Top Precambrian basement, H2: Top Paleozoic, H3: Top Cretaceous, H4: Top Paleogene, H5: Top Neogene). C- Interpreted geological profile with seismic units U1: Paleozoic, U2: Cretaceous, U3: Paleogene, U4: Neogene, U5: Quaternary.

El Caburé and Coronel Rico wells, U3 is located close to the surface.

Seismostratigraphic unit U4 (Figs. 6, 7) has high-amplitude reflectors, showing some stronger amplitude reflectors in the middle and lower sections of the unit with medium frequency, and strong lateral continuity. U4 contains parallel reflectors that are slightly curved upwards on top of the Pampeano-Chaqueño High. U4 has a general wedge-shaped geometry in the Northern Transect (Fig. 6), with much greater thickness in the west (~2000 ms TWT) than in the east (~300 ms TWT). In the Southern Transect (Fig. 7), U4 has an irregular and interrupted wedge shape, with a maximum thickness of 400 ms (TWT), locally decreasing or absent, as seen between the Quirquincho High and the Metán-Alemanía graben. The unit onlaps and covers the Quirquincho and Pampeano-Chaqueño highs.

Seismostratigraphic unit U5 (Figs. 6, 7) has medium to high-amplitude reflectors with high frequency and low continuity due to their near-surface location. Reflections within this unit are horizontal. The unit is generally tabular with a slight thickness increase to the west in the Northern Transect (Fig. 6); it has a gentle wedge shape in the Southern Transect (Fig. 7) with maximum thickness to the west and thins toward the east, where it eventually disappears.

4.1.3. *Chronostratigraphy and Lithology*

Based on biostratigraphic data recorded in the well reports (Pirané, Rolleri, 1965; Chirete, Pluspetrol, 1990; Las Breñas 1, Bottcher, 1974; Las Breñas 2, Rolleri, 1967; Las Breñas Oriental, Rolleri, 1966; Coronel Rico, Di Persia, 1969; El Caburé, Bottcher, 1965; Los Horcones 1, Di

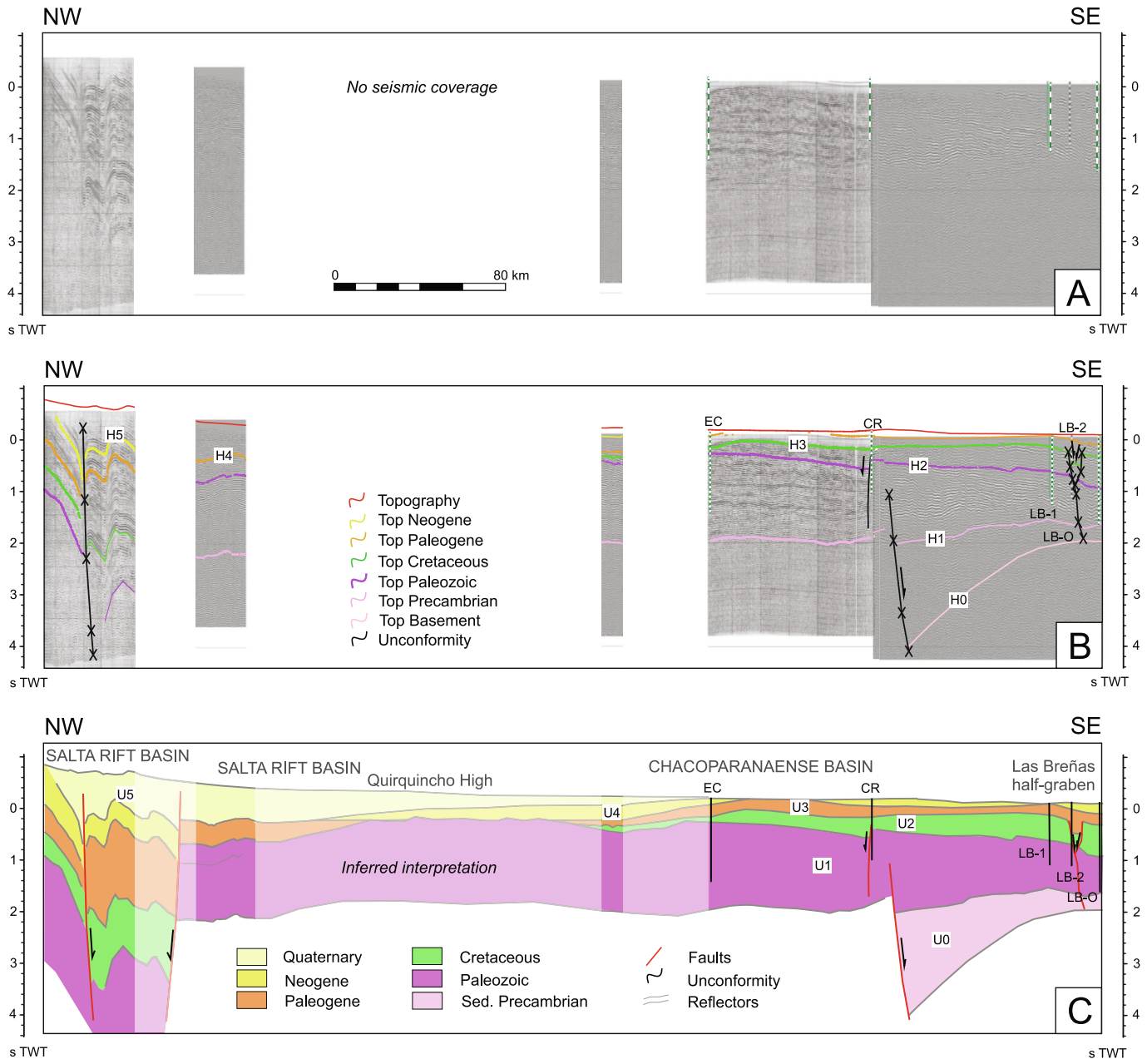

Fig. 7. NW-SE-oriented Southern Transect (ST) (see Fig. 5 for location). A- Uninterpreted seismic lines. B- Seismic profiles with interpreted color-coded horizons (H0: Local top basement - inferred, H1: Top Precambrian, H2: Top Paleozoic, H3: Top Cretaceous, H4: Top Paleogene, H5: Top Neogene). C- Interpreted geological profile across the seismic units U0: Precambrian metasediments, U1: Paleozoic, U2: Cretaceous, U3: Paleogene, U4: Neogene, U5: Quaternary. Interpreted data are shown in strong colours, extrapolated data are shown by transparent colors. Boreholes: EC-El Caburé, CR-Coronel Rico, LB1- Las Breñas 1, LB2- Las Breñas 2, LBO- Las Breñas Oriental.

Persia, 1970; Los Horcones 2, Moreno, 1973; Cerro Colorado, Pluspetrol, 1990) seismic units U1 to U5 correspond to Paleozoic (U1), Mesozoic – mainly Cretaceous– (U2), Paleogene (U3), Neogene (U4) and Quaternary (U5) sedimentary units.

Horizon H1 at the top of the acoustic basement corresponds to the top of Precambrian crystalline basement; except in the eastern sectors of the Southern Transect (Fig. 7), where Precambrian metasediments are represented by unit U0. Horizon H2 corresponds to the top of various Paleozoic units (Fig. 4) of the Chacoparanaense Basin and the adjacent Paleozoic Tarija Basin of southern Bolivia in the vicinity of the Salta Rift Basin area. The top of the Paleozoic unit (U1) contains marine clastic sedimentary rocks intercalated with diamictite beds.

Horizon H3 was penetrated by all wells and corresponds to the top of the Mesozoic (U2). The Mesozoic strata are mainly of Cretaceous age, whereas Triassic and Jurassic strata are absent in most of the basins (U2). According to the well reports, U2 in the Chacoparanaense Basin includes conglomerates, sandstones, and shale with limestone components, while in the Salta Rift Basin, U2 includes sandstones cemented by calcite and limestones.

Horizon H4 is the top of the Paleogene unit (U3); it comprises continental sandstones in the Chacoparanaense Basin, as well as fluvial and lacustrine sandstones and shale in the Salta Rift Basin. Horizon H5 top-bounds the Neogene units (U4); this unit contains shale and sandstones in the Chacoparanaense Basin; and sandstones, siltstones, and conglomerates in the Salta Rift Basin. The Quaternary sediments (U5) at the top of the stratigraphic succession mostly consist of unconsolidated fluvial clastic rocks (conglomerates, sandstones, siltstones, claystones). The coarsest strata are part of alluvial-fan deposits that cover the

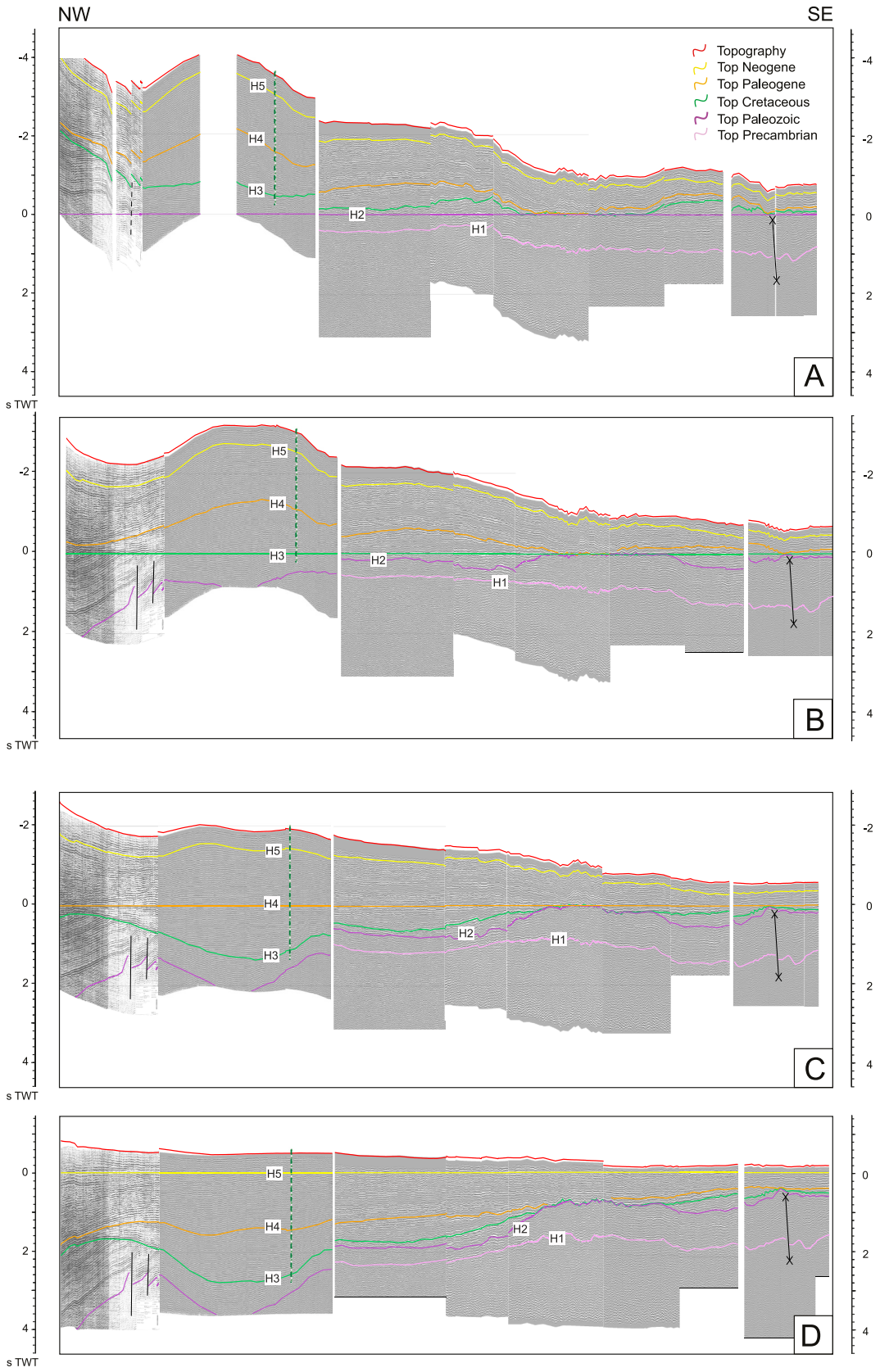

Fig. 8. Flattening of the horizons in the Northern Transect (see location in Fig. 5). A- Flattening of H2-Top Paleozoic. B- Flattening of H3-Top Cretaceous. C- Flattening of H4-Top Paleogene. D- Flattening of H5-Top Neogene.

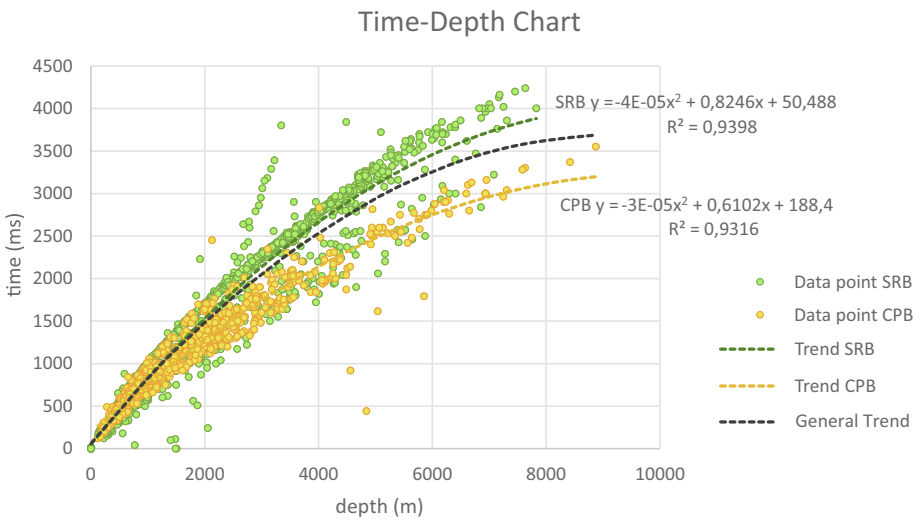

Fig. 9. Time–depth chart for the wells and seismic profiles of the Salta Rift (SRB) and Chacoparanaense Basins (CPB). Each data point corresponds to one check-shot. Three trends and equations are generated from the data: an SRB trend for the Salta Rift Basin, a CPB trend for the Chacoparanaense Basin, and a general trend for the entire study area.

sediments of the Salta Rift Basin. Finer-grained sandstone-to-clay units mark the distal areas of the Chacoparanaense Basin.

4.2. Flattening of horizons

Flattening of H2 – Paleozoic Top – (Fig. 8A) shows how the horizon below (H1) is approximately horizontal, exhibiting a slight depression in the area of the metasediments of the Quirquincho High. The horizons above H3 and H4 record onlap terminations toward H2 in the region of the Pampeano-Chaqueño and Quirquincho highs. Flattening of H3 –Top Cretaceous – (Fig. 8B) emphasizes the onlap on H2 in the area of both highs and illustrates how H4 –Top Paleogene- terminates in an onlap contact with respect to H2 and H3. Flattening of H4 – Top Paleogene – (Fig. 8C) displays onlap terminations on H2 and H3 in the region of the Pampeano-Chaqueño and Quirquincho highs. To the west, H3 exhibits a depocenter with a graben, whose bounding faults also affect the top of H2; this area corresponds to the Lomas de Olmedo depocenter of the Salta Rift Basin. Flattening of H5 – Top Neogene – (Fig. 8D) resembles the original Northern Transect (Fig. 6). The most notable feature is the westward-thickening wedge shape of the Neogene sedimentary units.

4.3. Thematic maps

4.3.1. Depth maps

The depth of the Precambrian Top (Fig. 10A) varies from 1650 m below sea level (b.s.l.) to ~9150 m b.s.l. The deepest sector is located northwest of the study area within the Lomas de Olmedo depocenter of the Salta Rift. In the Metán-Alemanía subbasin on its western margin, the depth reaches 6300 m b.s.l. The depth of the horizon decreases toward the southeast, showing two elevated areas with approximately NE-SW-orientation. The first of these is located around the north-central part of the study area and coincides with the position of the Quirquincho High. The second, located close to the eastern boundary of the study area, is clearly associated with the location of the Pampeano-Chaqueño High.

The Paleozoic Top (Fig. 10B) ranges from 250 m above sea level (a.s.l.) to 7550 m b.s.l., with its maximum depth northwest of the study area, where the Paleozoic rocks underlie the Lomas de Olmedo depocenter of the Salta Rift (Fig. 3). The depth of this horizon decreases toward an elevated area in the center of the map; this area is approximately 150 km wide and oriented NE-SW. To the east, parts of the main elevated area are still visible at the Paleozoic Top, coinciding with the location of the Pampeano-Chaqueño High; however, not as prominently as in the horizon below.

The Cretaceous Top (Fig. 10C) lies at a depth, ranging from 45 m a.s.l. to 6230 m b.s.l. The area with the greatest depth is located in the northwest, from which it progressively rises toward its highest elevations in the southern region of the study area.

The depth of the Top Paleogene (Fig. 10D) ranges from 630 m a.s.l. to 3260 m b.s.l. The deepest area is located to the northwest, and the depth decreases gradually toward the southeast, except for a few sectors with minor elevations in the southwest, where Cenozoic mountain ranges exist and are associated with folding and inversion of structures.

4.3.2. Isopach maps

The thickness distribution of the Paleozoic unit (U1) ranges from 0 m to 4360 m (Fig. 11A). U1 is thinnest or undetectable in the northwest, located approximately beneath the Lomas de Olmedo depocenter of the Salta Rift Basin, because the Precambrian basement is too deep in this area for a reliable identification in seismic profiles. In addition, in some regions, it is not possible to distinguish between the Paleozoic rocks and the Precambrian basement in the seismic interpretations because H1 is too deep. The three areas with the greatest sediment thickness are located in the southwest, to the east, and in the Las Breñas half-graben. The first, larger area has an irregular thickness distribution, whereas the second area corresponds to the normal-fault offset of the basement surface near the Pampa Bandera well. (Las Breñas half-graben). To the west of this area lies an elongated region of reduced sediment thickness with NE-SW-orientation. This area corresponds to the position of the Pampeano-Chaqueño High. The third region is a small sector in the north, but this could be the result of an artifact, as the H1 Basement top could not be interpreted using seismic data. This region is characterized by medium-thickness sediments (Fig. 11A).

The thickness of the Cretaceous unit (U2) (Fig. 11B) ranges from 0 m to 2300 m; its thickest sector is located to the northwest, coinciding with the Salta Rift Basin. The thinnest area is elongated and located in the center of the analyzed area; It corresponds to the Quirquincho High.

The thickness of the Paleogene unit (U3) (Fig. 11C) spans 0 m to 3000 m. The thickest region is to the northwest, with decreasing thickness toward the southeast, reaching almost zero thickness in nearly half of the study area. There are some irregular distributions of sedimentary units in the southwest, in the area of the Cenozoic La Candelaria Range (Santa Bárbara System, Fig. 1) (Arnous, 2021; Arnous et al., 2024). This sedimentary unit generally has the shape of a wedge, being

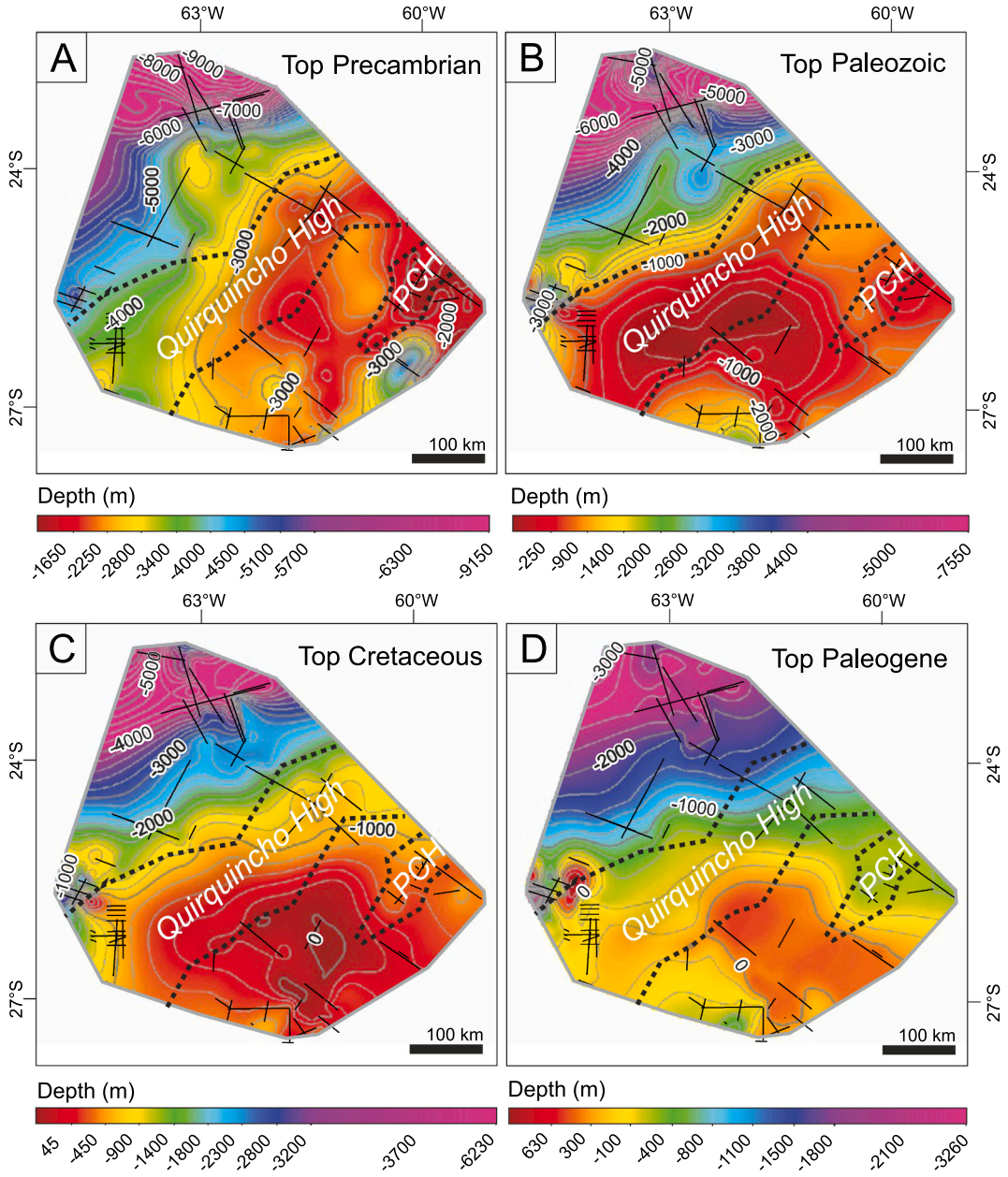

Fig. 10. Depth map depicting the present-day subsurface position and morphology of the top of each stratigraphic unit of horizons 1 to 4: A) H1- Precambrian Top, B) H2- Paleozoic Top, C) H3- Cretaceous Top, D) H4- Paleogene Top. Seismi- line locations are shown as black lines.

thicker to the northwest and pinching out toward the southeast.

The thickness of the Neogene unit (U4) (Fig. 11D) ranges from 0 m to 4200 m, with greater values in the northwest and a gradual decrease toward the southeast. Similar irregularities in thickness distribution were observed with regard to the Paleogene units in the southwest. The Neogene exhibits comparable features, but a generally gentler wedge shape than what could be inferred from the Paleogene isopach map.

5. Geological interpretation

The stratal terminations and thickness variations in the seismic transects across the basement highs constrain the timing of the development of the Quirquincho and Pampeano–Chaqueño highs. In the Northern Transect, H1 (Precambrian Top) and H2 (Paleozoic Top) form an antiformal structure at the Quirquincho High (Fig. 6). The U1 (Paleozoic) is truncated at the top by an unconformity (Fig. 12). The Cretaceous (U2) and Paleogene (U3) units onlap the flanks of the Quirquincho High and thin progressively toward the center of the structure until they disappear at the crest (Fig. 12).

Flattening of the Top Cretaceous horizon H3 (Fig. 8B) shows that the Paleozoic unit (U1) formed a paleo-high during Cretaceous deposition, with sedimentary onlap on both flanks. Flattening of the Top Paleogene horizon (Fig. 8C) reveals that the Quirquincho High continued to stand out as a positive feature during the Paleogene, with sediment again onlapping its flanks. On the Cretaceous isopach map (Fig. 11B), sediment thickness diminishes to <200 m or disappears altogether above the high. The Top Paleozoic depth map (Fig. 10B) also exhibits positive relief relative to adjacent areas.

The combination of i) stratigraphic and structural seismic interpretation, ii) horizon flattening, and iii) depth and thickness reconstructions document that the Quirquincho High was part of the depositional area during most of the Paleozoic, but evolved into a positive topographic feature during the late Paleozoic, Mesozoic and early Paleogene. Truncation of Paleozoic reflectors (Figs. 6, 12) indicates

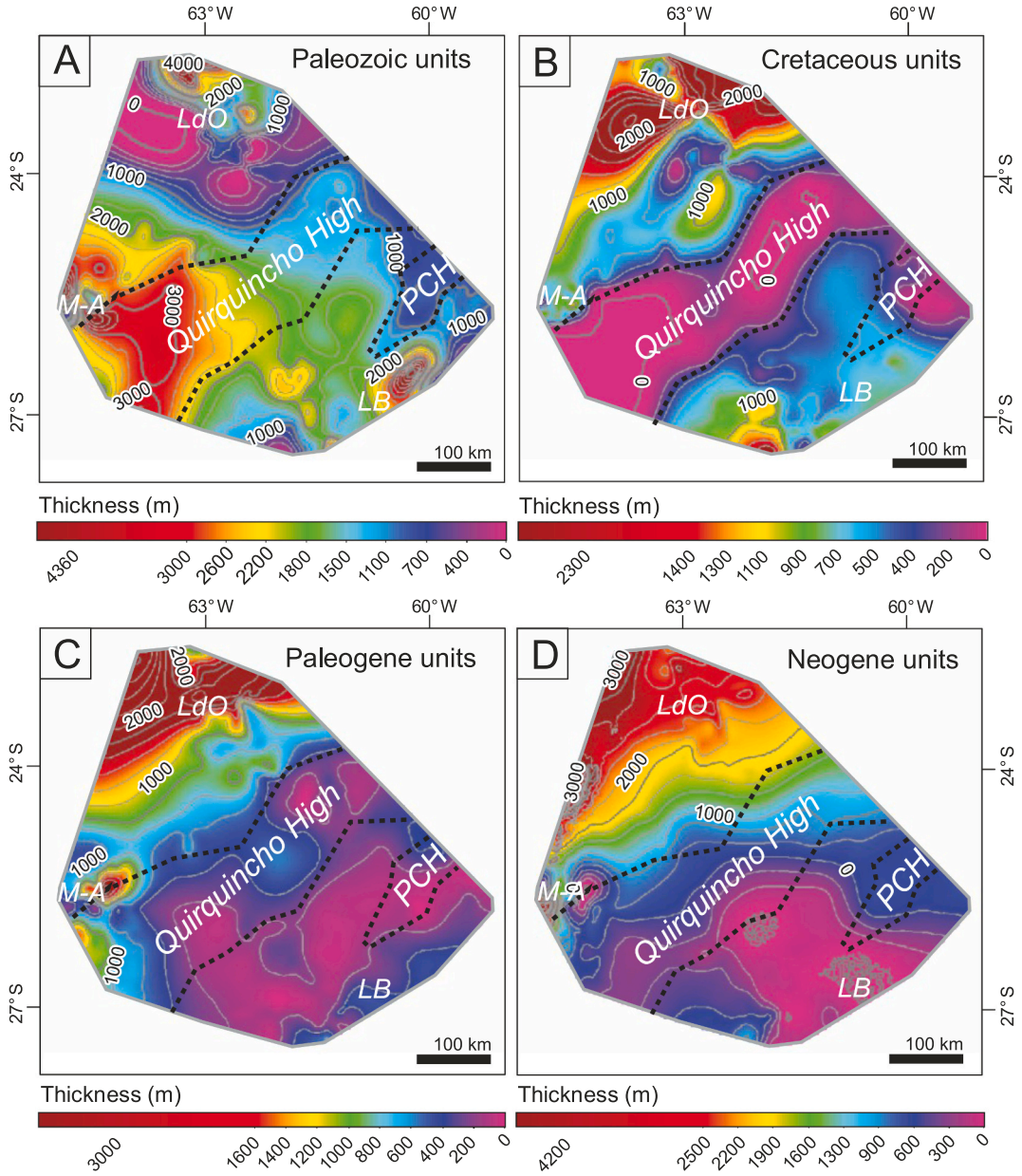

Fig. 11. Thickness distribution of units 1 to 4: A) U1-Paleozoic sediments, B) U2-Cretaceous sediments, C) U3-Paleogene sediments, D) U4-Neogene sediments. Location of the main structures: Lomas de Olmedo depocenter, LdO; Metàn-Alemanìa depocenter, M-A; Las Breñas halfgraben, LB; Quirquincho High; Pampeano-Chaqueño High, PCH.

erosional exhumation, whereas Cretaceous and Paleogene reflectors onlap against the high. Thickness variations suggest that basement uplift diminished gradually and ceased during the latter part of Paleogene; subsequently, Neogene and Quaternary units were deposited without interruption, ultimately burying the structure. These observations establish the relative timing of uplift; the possible tectonic mechanisms responsible are discussed below.

At the eastern end of the Northern Transect (Fig. 6), H1 (Precambrian Top) and H2 (Paleozoic Top) are elevated beneath the Pampeano–Chaqueño High. Paleozoic unit (U1) exhibits reflector folding, and an east-dipping normal fault cuts both Precambrian and Paleozoic levels. The overlying Mesozoic strata (U2) are thin and display folded and truncated reflectors that may indicate growth strata (Fig. 12). Near the top of the high, Paleogene strata (U3) onlap both flanks, with truncation and onlap marking the unconformity. The Top Precambrian depth map (Fig. 10A) depicts the Pampeano–Chaqueño High as an irregular, NE–SW–oriented area of uplift. It is smaller in extent and elevation than the Quirquincho High. The Paleozoic isopach map (Fig. 10A) reveals thinning above the structure, indicating the influence of positive relief during Paleozoic sedimentation. The Cretaceous and Paleogene isopach maps (Fig. 11B–C) also reveal thinning of strata near the high, consistent with onlap geometries. Above this succession, Neogene and Quaternary units form tabular reflectors that fully bury the structure. These relationships establish that the Pampeano–Chaqueño High influenced deposition from the late Paleozoic through the Paleogene, but had no effect on Neogene and Quaternary sedimentation patterns.

In the Southern Transect (Fig. 7), we interpreted the Quirquincho High to have a morphology similar to that observed in the Northern Transect. However, Cretaceous sediments do not extend west of the high into the southwestern Salta Rift Basin. There, the Cretaceous unit is bounded by two N–S-striking normal faults (Cristallini et al., 1997; Iaffa et al., 2013) that form the Metán–Alemanía depocenter (Fig. 7). These faults affect the basement and all overlying units, with thickened

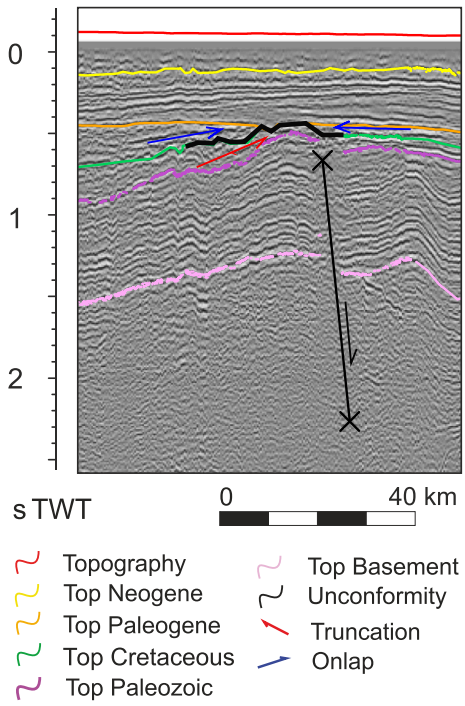

Fig. 12. Detail of the seismic interpretation of the Northern Transect (see Fig. 6 for location) showing stratal terminations, along the unconformity at the Pampeano-Chaqueño High.

Cretaceous and Paleogene sections within the graben. However, faults start to invert during the late Paleogene; Neogene strata record no growth geometries in the graben, but are folded along with the underlying units, indicating reactivation and contractional inversion of the faults during Andean compression. Quaternary strata cover the former rift-shoulder areas. To the north, the Lomas de Olmedo depocenter differs in structural style and is bounded by E–W-striking faults, which controlled inversion during Cenozoic shortening (Kley et al., 2005; Iaffa et al., 2011), with evidence faulting during the Holocene (Ramos et al., 2006).

Flattening of the Top Neogene horizon H5 (Fig. 8D) reveals a major westward-thickening wedge geometry typical for a foreland basin, reflecting flexural subsidence driven by Andean loading (Horton and Folguera, 2019). Quaternary sediments display a similar wedge geometry, beginning farther east in the Southern Transect. In the western Metán–Alemanía depocenter, Neogene sediments are folded and exposed at the surface, whereas Quaternary deposits are less deformed and crop out farther east, reflecting continued shortening in the Eastern Cordillera (e.g., Garcia et al., 2019; Figueroa et al., 2021; Elías, 2025).

6. Discussion

6.1. Conceptual models regarding the evolution of the basement highs

Our analysis indicates that the Quirquincho and Pampeano–Chaqueño highs were positive features from the late Paleozoic onward, influencing sedimentation patterns in the Mesozoic and the Paleogene. There are currently several hypotheses for the origin of these two prominent subsurface features, which we will discuss below.

Basement highs in distal foreland regions may occur in a range of tectonic settings and may therefore be caused by a range of geological processes (Peacock and Banks, 2020). At first sight, one feasible possibility is that the Quirquincho and Pampeano–Chaqueño highs represent forebulges in the Cenozoic Andean flexural foreland system (DeCelles and Giles, 1996). In such a scenario the Quirquincho High could have formed during Andean tectonic loading starting in the Paleogene (Horton, 2018; Coutand et al., 2001). Similarly, in this context the Pampeano–Chaqueño High might represent a younger Neogene forebulge, implying eastward migration of flexural subsidence. However, our seismic data reveal a lack of contractional deformation in the Cenozoic cover units. The timing of uplift inferred from unconformities predates the Paleogene and is therefore not compatible with the influence of Cenozoic Andean tectonism. A Cenozoic forebulge, however, exists in the Andean Foreland Basin approximately west of 60° W (e.g., McGlue et al., 2016) and influences hydrological, geomorphic, and sedimentary processes (Repasch et al., 2021, 2023).

The second hypothesis for the origin of the Quirquincho and Pampeano–Chaqueño highs is their evolution as rift shoulders during Mesozoic extension associated with the formation of the Salta Rift (Salfity and Marquillas, 1994; Starck, 2011). Comparable rift-shoulder uplift of large regional extent is known from the Atlantic margin of North America (Anell et al., 2009), the Rona Ridge in the UK (Trice, 2014), and the Kenya and Ethiopian rifts (Foster and Gleadow, 1996; Torres Acosta et al., 2015; Boone et al., 2019). Unlike those cases, however, our data show no *syn*-rift thickening or bounding normal faults at the highs. Furthermore, given the typical spatial relationships between graben formation and rift-shoulder uplift (e.g., Allen and Allen, 2013) the Pampeano-Chaqueño high is far too distant from the Salta Rift to be caused by it. This temporal, spatial, and structural mismatch indicates that a simple rift-shoulder model is not applicable here.

The third explanation for the formation of the highs is the activity of blind thrusts or reverse faults, associated with a major, westward-dipping crustal detachment which might have been active during the early stages of development of the Chacoparanaense Basin. However, although such structures are common in the adjacent broken foreland (Kley et al., 2005; Iaffa et al., 2011, 2013; Arnous et al., 2024), we were unable to observe any evidence for such large-scale tectonic structures in our study area to support this alternative interpretation.

Importantly, the analysis of the unconformities and lateral pinchouts and terminations, as well as the general morphology of the Quirquincho and Pampeano-Chaqueño basement highs, suggests that both structures were formed during the late Paleozoic and are thus paleo-tectonic relic features that continued to exert influence on subsequent sedimentary processes. The data analyzed confirm that the Chacoparanaense Basin was a subsiding area with epicontinental marine sedimentation during the late Precambrian and early Paleozoic (Russo et al., 1979; Chebli et al., 1999). In this context, another alternative for the formation of the Quirquincho and Pampeano-Chaqueño basement highs is that their uplift was caused by flexural loading induced by the growth of the ancient Andes (*sensu* Limarino et al., 2023) during the Gondwanan orogeny along the western margin of Gondwana. This orogeny lasted from the Carboniferous to the Permian, and perhaps continued during the early Triassic (Ramos, 1999; Heredia et al., 2016, 2018; Limarino et al., 2023). In such a geodynamic setting the Quirquincho and Pampeano-Chaqueño highs might represent remnants of ancient Paleozoic forebulges that developed during the eastward migration of the Gondwanan deformation front (Fig. 14). Chronologically, this event is indicated by the truncation of the Paleozoic strata below the Top Paleozoic unconformity, and by the onlap terminations of Mesozoic and Paleogene seismic units against the underlying Paleozoic units (Figs. 6, 7, 8, 12, 13).

In the Paleozoic forebulge scenario, tectonic processes in the Gondwanan orogen could have caused the deformation of the continental lithosphere involving the successive development of two forebulges during the migration of the crustal flexural response due to tectonic loading (Fig. 14). The first, older and larger forebulge was the Quirquincho High, whereas the second, younger and smaller forebulge, was the Pampeano-Chaqueño High. The Pampeano-Chaqueño High might have formed by eastward flexural migration in combination with the presence of a mechanically weaker, lower crustal density zone (e.g., Meeßen et al., 2018) that was conducive to deformation far away from the Gondwanan deformation front.

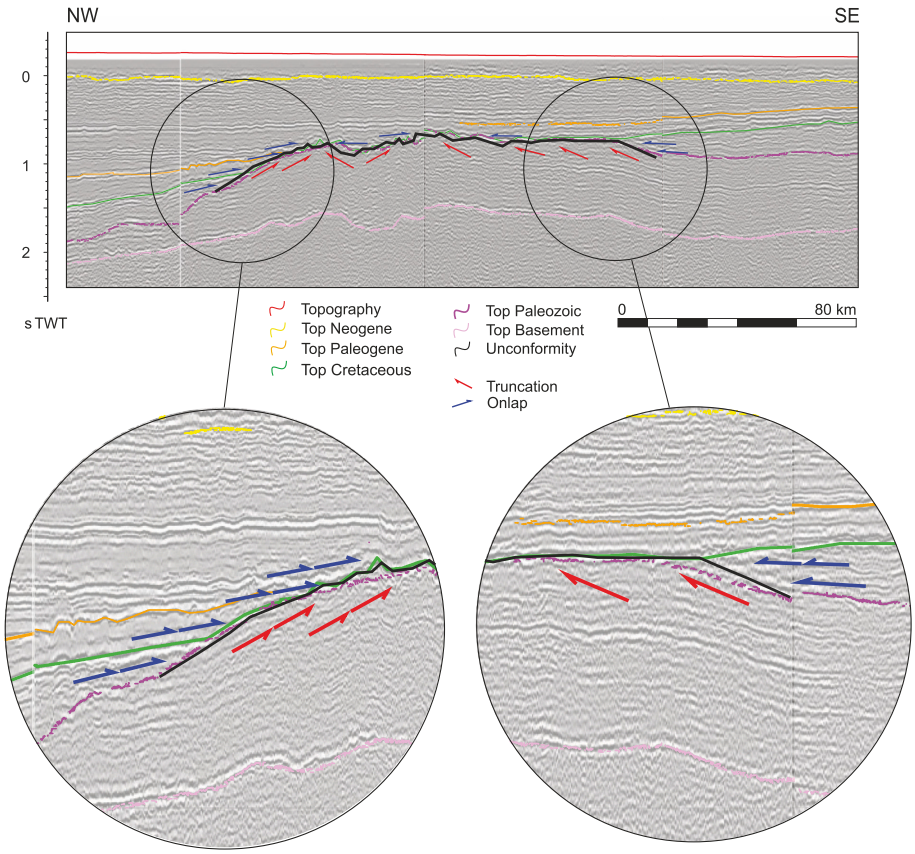

Fig. 13. Detail of the seismic interpretation of the Northern Transect (see Fig. 6 for location) showing stratal terminations, along the unconformity at the Quirquincho High.

6.2. Influence of the basement highs and comparison with the Cenozoic Andean foreland

The identification of possible Paleozoic forebulge relics in the Chacoparanaense basin documents the influence of inherited, deep-seated crustal structures on modern basin evolution. During the Gondwanan orogeny, the South American plate underwent thin-skinned flexural deformation (Heredia et al., 2016, 2018; Limarino et al., 2023) that produced a classical foreland system (e.g., DeCelles and Giles, 1996). This system included a wedge-top (preserved in the modern Frontal Cordillera; Limarino et al., 2023), a foredeep (e.g., Paganzo, Tarija, and San Rafael basins, Limarino et al., 2023), a forebulge (represented by the Quirquincho and Pampeano-Chaqueño highs), and a backbulge zone (represented by the Chacoparanaense Basin).

In contrast, the Cenozoic Andean foreland above this old tectonic system is a broken foreland, lacking a continuous depozone architecture and dominated by thick-skinned deformation (Ramos et al., 2006; Iaffa et al., 2011; Strecker et al., 2011; Del Papa et al., 2013; Zapata et al., 2020). Unlike the relic structural highs, which show stratigraphic thinning and onlap, the Cenozoic structural archives record inversion of inherited rift faults and basement uplifts. This is in stark contrast to the buried Paleozoic foreland-basin system, emphasizing, how crustal inheritance - particularly with respect to structures developed during the Mesozoic Salta Rift phase - transformed and pre-conditioned a formerly contiguous Paleozoic lowland region into a compartmentalized Cenozoic foreland.

Recent global syntheses document that continuous and broken forelands form depending on lithospheric strength and inherited structures (e.g., Lacombe and Bellahsen, 2016; Watts, 2001). The contrast between the Paleozoic, flexurally driven continuous foreland and the Cenozoic broken foreland in northwestern Argentina, as interpreted in this study, illustrates this principle. The Quirquincho and Pampeano–Chaqueño highs originated as flexural forebulges during the Paleozoic, building the structural foundation of the Chacoparanaense Basin (Figs. 3, 6, 7). Mesozoic extension farther west did not affect these deep-seated structures. Cenozoic Andean tectonics resulted in thick-skinned inversion of rift faults in the proximal (Salta) part of the modern Andean foreland. These processes had a far-field influence on the study area as the Quirquincho and Pampeano–Chaqueño highs were peripherally affected by a general westward basin tilt due to tectonic loading by the Cenozoic Andes.

There are several analogs from other regions that highlight how forebulges can be preserved in the stratigraphic record. For example, the Iquitos Arch in the Amazonian foreland (Roddaz et al., 2005) resembles the Quirquincho High in acting as an inherited flexural high that subsequently influenced sediment dispersal. In contrast, the Apulian forebulge of the Adriatic Sea underwent syn-contractional deformation (Billi and Salvini, 2003), which is absent in our case. Paleozoic and Mesozoic examples, such as the Alleghanian forebulge (Lash and Engelder, 2007) and the Laramide forebulge (White et al., 2002), typically display unconformities and stratal thinning comparable to those documented around the Quirquincho and Pampeano–Chaqueño highs. In another example, the Ediacaran forebulge grabens of the São Francisco Basin (Reis et al., 2017) provide an even older analog of inherited structural influence on foreland sedimentation, supporting the notion that flexural uplifts may persist as geomorphic entities across multiple tectonic phases. These comparisons reinforce that the truncation, onlap, and thinning we observed correspond to the diagnostic features of forebulge unconformities as described in foreland-basin and sequence-stratigraphic syntheses (e.g., DeCelles and Giles, 1996; Crampton and Allen, 1995; Catuneanu, 2004).

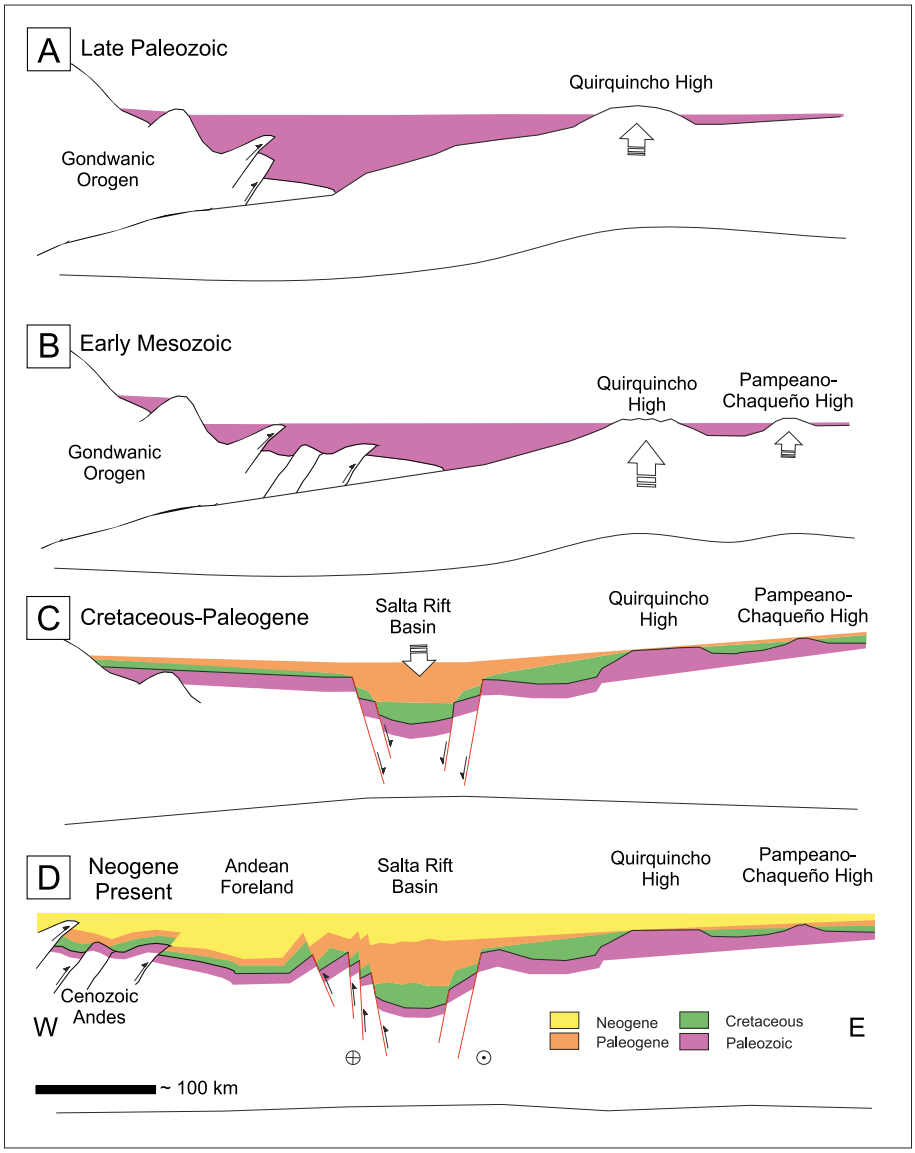

Fig. 14. Conceptual model of the evolution of the Quirquincho and Pampeano-Chaqueño highs. A) Late Paleozoic: development of the Quirquincho High. B) Early Mesozoic: development of the Pampeano-Chaqueño High and erosion on the Quirquincho High. C) Cretaceous-Paleogene: Development of the Salta Rift Basin and onlapping strata on high topography. D) Neogene: Setting of the Andean Foreland Basin, progressive inversion of inherited normal faults, and complete covering of the inherited topographic highs by Neogene and Quaternary sediments.

7. Conclusions

The subsurface conditions of the Chacopampean Plain and long-term sediment deposition in the area of the present-day foreland of the Andes are strongly influenced by the topography of inherited Paleozoic basement highs. The Quirquincho High records uplift and stratal terminations consistent with a forebulge formed during late Paleozoic Gondwanan orogenesis. The Pampeano–Chaqueño High farther east represents a second, areally more limited Paleozoic forebulge that likely developed subsequently in a region of inherited crustal weakness. Both features remained positive topographic elements throughout the Mesozoic, guiding sediment distribution and the formation of onlaps as the region became part of the greater Salta Rift province. Both structures were ultimately buried beneath the Cenozoic Andean foreland deposits, when renewed tectonism related to the subduction of the Nazca plate beneath South America affected the foreland. During this episode of basin evolution contractional deformation in the foreland inverted parts of the Salta Rift Basin, while the Quirquincho and Pampeano–Chaqueño highs were progressively buried and slightly tilted to the west, which caused the wedge-shaped accumulation of sediments during the Cenozoic.

This study highlights the long-term influence of inherited Paleozoic forebulges on the tectono-sedimentary evolution of the Andean foreland in northern Argentina, demonstrating how basement features can persist through multiple tectonic episodes, exerting a far-reaching influence on the structural and stratigraphic architecture of foreland basins.

CRediT authorship contribution statement

Valentina Cortassa: Writing – original draft, Investigation, Formal analysis, Data curation. **Stefan Back:** Software, Methodology, Data curation. **Robert Ondrak:** Writing – review & editing, Supervision, Funding acquisition. **Cecilia del Papa:** Writing – review & editing, Supervision. **Eduardo Rossello:** Supervision, Resources, Funding acquisition, Conceptualization. **Manfred R. Strecker:** Writing – review & editing, Supervision.

Declaration of competing interest

The authors declare that they have no known competing financial interests or personal relationships that could have appeared to influence the work reported in this paper.

Acknowledgments

This research was funded by CONICET (Consejo Nacional de Investigaciones Científicas y Técnicas, Argentina), by the international cooperation program StRATEGy of the German Science Foundation (DFG; STR 373/34-1) between Germany and Argentina (Surface Processes, Tectonics and Georesources: The Andean Foreland Basin of Argentina), and the German Ministry of Science and Technology (BMBF) project DeArGeonet. Access to analog subsurface data (2D seismic lines and well logs) was provided by BHP Petroleum Argentina S.A. We thank Schlumberger S.A. for providing the Petrel software; S&P Global for providing KingdomSuite software; and Philipp Konerding for providing the kogeo seismic toolkit. We sincerely thank Michal Nemčok for thorough and constructive reviews of earlier versions of this manuscript, an anonymous second reviewer for valuable comments, and editors Piotr Krzywiec and Liviu Matenco for their suggestions.

Data availability

The data used to produce this publication is available in the following data repository: https://doi.org/10.5880/fidgeo.2025.038.

References

Allen, P.A., Allen, J.R., 2013. Basin Analysis: Principles and Application to Petroleum Play Assessment, third ed. John Wiley & Sons, Oxford.

Allmendinger, R.W., Jordan, T.E., Kay, S.M., Isacks, B.L., 1997. The evolution of the Altiplano – Puna plateau of the Central Andes. Annu. Rev. Earth Planet. Sci. 25, 139–174. https://doi.org/10.1146/annurev.earth.25.1.139.

Anell, I., Thybo, H., Artemieva, I.M., 2009. Cenozoic uplift and subsidence in the North Atlantic region: geological evidence revisited. Tectonophysics 474, 78–105. https://doi.org/10.1016/j.tecto.2008.06.015.

Arnous, A., 2021. Paleosismología y neotectónica del antepaís fragmentado en el extremo sureste del Sistema Santa Bárbara, Noroeste Argentino. Doctoral dissertation. Universität Potsdam.

Arnous, A., Garcia, V.H., Pingel, H., Giambiagi, L., Strecker, M.R., 2024. Kinematic evolution of the Santa Barbara System in the foreland of the Central Andes of northwestern Argentina (26°S). Tectonics 43, e2023TC008195. https://doi.org/10.1029/2023TC008195.

Billi, A., Salvini, F., 2003. Development of systematic joints in response to flexure-related fibre stress in flexed foreland plates: the Apulian forebulge case history, Italy. J. Geodyn. 36, 523–536. https://doi.org/10.1016/S0264-3707(03)00049-3.

Blisniuk, P.M., Sonder, L.J., Lillie, R.J., 1998. Foreland normal fault control on NW-Himalayan thrust front development. Tectonics 17, 766–779. https://doi.org/10.1029/98TC01438.

Bookhagen, B., Strecker, M.R., 2008. Orographic barriers, high-resolution TRMM rainfall, and relief variations along the eastern Andes. Geophys. Res. Lett. 35, L06403. https://doi.org/10.1029/2007GL032011.

Boone, S.C., Balestrieri, M.L., Kohn, B.P., Corti, G., Gleadow, A.J.W., Seiler, C., 2019. Tectonothermal evolution of the Broadly Rifted Zone, Ethiopian Rift. Tectonics 38, 1070–1100. https://doi.org/10.1029/2018TC005210.

Bottcher, G., 1965. Stratigraphy Report of the Well YPF.SE.EC.x-1 (Santiago del Estero, Argentina). YPF S.A., unpublished results).

Bottcher, G., 1974. Stratigraphy Report of the Well YPF.CHA.LB-1 (Chaco, Argentina). YPF S.A., unpublished results.

Campos, H., Mann, P., 2015. Tectonostratigraphic evolution of the Northern Llanos Foreland Basin of Colombia and implications for its hydrocarbon potential. J. South Am. Earth Sci. 59, 101–116. https://doi.org/10.1016/j.jsames.2014.12.002.

Carrapa, B., Adelmann, D., Hilley, G., Mortimer, E., Strecker, M.R., Sobel, E.R., 2005. Oligocene uplift, establishment of internal drainage and development of plateau morphology in the southern Central Andes. Tectonics 24, TC4011. https://doi.org/10.1029/2004TC001719.

Carrapa, B., Bywater-Reyes, S., DeCelles, P.G., Mortimer, E., Gehrels, G.E., 2012. Late Eocene-Pliocene basin evolution in the Eastern Cordillera of northwestern Argentina (25°–26° S): regional implications for Andean orogenic wedge development. Basin Res. 24, 249–268. https://doi.org/10.1111/j.1365-2117.2011.00530.x.

Carrera, N., Muñoz, J.A., 2008. Thrusting evolution in the southern Cordillera Oriental (northern Argentine Andes): constraints from growth strata. Tectonophysics 459, 107–122. https://doi.org/10.1016/j.tecto.2007.12.015.

Carrera, N., Muñoz, J.A., Sábat, F., Mon, R., Roca, E., 2006. The role of inversion tectonics in the structure of the Cordillera Oriental (NW Argentinean Andes). J. Struct. Geol. 28, 1921–1932. https://doi.org/10.1016/j.jsg.2006.07.009.

Catuneanu, O., 2004. Retroarc foreland systems – evolution through time. J. Afr. Earth Sci. 38, 225–242. https://doi.org/10.1016/j.jafrearsci.2003.11.002.

Cediel, F., Shaw, R.P., Cáceres, C., 2003. Tectonic assembly of the northern Andean Block. In: Bartolini, C., Buffler, R.T., Blickwede, J. (Eds.), The Circum-Gulf of Mexico and the Caribbean: Hydrocarbon Habitats, Basin Formation, and Plate Tectonics, AAPG Memoir, vol. 79, pp. 815–848.

Chebli, G., Mozetic, M., Rossello, E., Bühler, M., 1999. Cuencas sedimentarias de la llanura Chacopampeana. In: Caminos, R. (Ed.), Geología Argentina, Anales, 29. Subsecretaría de Minería de la Nación, Buenos Aires, pp. 627–644.

Cloetingh, S.A.P.L., Burov, E., Matenco, L., Toussaint, G., Bertotti, G., Andriessen, P.A.M., Wortel, M.J.R., Spakman, W., 2004. Thermo-mechanical controls on the mode of continental collision in the SE Carpathians (Romania). Earth Planet. Sci. Lett. 218, 57–76. https://doi.org/10.1016/S0012-821X(03)00599-2.

Cobbold, P.R., Rossello, E.A., Roperch, P., Arriagada, C., Gómez, L.A., Lima, C., 2007. Distribution, timing, and causes of Andean deformation across South America. In: Ries, A.C., Butler, R.W.H., Graham, R.H. (Eds.), Deformation of the Continental Crust: The Legacy of Mike Coward, Geol. Soc. Lond. Spec. Publ, vol. 272, pp. 321–343. https://doi.org/10.1144/GSL.SP.2007.272.01.17.

Cortassa, V., Rossello, E., Back, S., del Papa, C., Ondrak, R., Strecker, M., 2022. Subsurface basement topography in the Cenozoic Andean foreland basin of northern Argentina. EGU General Assembly 2022. https://doi.org/10.5194/egusphere-egu22-13302. EGU22-13302.

Cortassa, V., Back, S., Ondrak, R., del Papa, C., Strecker, M., Rossello, E., 2025. Subsurface data from the Chacopampean plain, North Argentina [dataset]. GFZ Data Services. doi:10.5880/fidgeo.2025.038.

Coutand, I., Cobbold, P.R., de Urreiztieta, M., Gautier, P., Chauvin, A., Gapais, D., Rossello, E.A., López-Gamundí, O., 2001. Style and history of Andean deformation, Puna plateau, northwestern Argentina. Tectonics 20, 210–234. https://doi.org/10.1029/2000TC001221.

Crampton, S.L., Allen, P.A., 1995. Recognition of forebulge unconformities associated with foreland flexure. AAPG Bull. 79, 1495–1514. https://doi.org/10.1306/D3926B93-2A99-11D7-8645000102C1865E.

Cristallini, E., Cominguez, A.H., Ramos, V.A., 1997. Deep structure of the Metan-Guachipas region: Tectonic inversion in northwestern Argentina. J. South Am. Earth Sci. 10 (5–6), 403–421. https://doi.org/10.1016/S0895-9811(97)00026-6.

DeCelles, P.G., 2011. Foreland basin systems revisited: variations in response to tectonic settings. In: Busby, C., Pérez, A.A. (Eds.), Tectonics of Sedimentary Basins: Recent Advances. Wiley-Blackwell, Chichester, pp. 405–426. https://doi.org/10.1002/9781444347494.ch19.

DeCelles, P.G., Giles, K.A., 1996. Foreland basin systems. Basin Res. 8, 105–123. https://doi.org/10.1046/j.1365-2117.1996.00192.x.

Del Papa, C., Hongn, F., Powell, J., Payrola, P., Do Campo, M., Strecker, M.R., Pereyra, R., 2013. Middle Eocene-Oligocene broken-foreland evolution in the Andean Calchaqui Valley, NW Argentina. Basin Res. 25, 574–593. https://doi.org/10.1111/bre.12028.

Di Persia, C.A., 1969. Stratigraphy Report of the Well YPF.SE.CR.x-1 (Santiago del Estero, Argentina). YPF S.A., unpublished results.

Di Persia, C.A., 1970. Stratigraphy Report of the Well YPF.SE.LH.x-1 (Santiago del Estero, Argentina). YPF S.A., unpublished results.

Elías, L.I., 2025. Evolución tectónica plio–cuaternaria de la Cordillera Oriental entre los 25° y 25° 35'S. Doctoral dissertation. Universität Potsdam.

Escalona, A., Mann, P., 2006. An overview of the petroleum system of Maracaibo Basin. AAPG Bull. 90, 657–678. https://doi.org/10.1306/11100505096.

Favetto, A., Rocha, V., Pomposiello, C., García, R., Barcelona, H., 2015. A new limit for the NW Río de la Plata Craton Border at about 24°S (Argentina) detected by Magnetotellurics. Geol. Acta 13, 243–254. https://doi.org/10.1344/GeologicaActa2015.13.3.6.

Fernández Garrasino, C., Laffitte, G., Villar, H., 2005. Cuenca Chacoparanaense. In: 6° Congreso de Exploración y Desarrollo de Hidrocarburos. Frontera Exploratoria de la Argentina, Mar del Plata, pp. 97–114.

Figueroa, S., Weiss, J.R., Hongn, F., Pingel, H., Escalante, L., Elías, L., Strecker, M.R., 2021. Late Pleistocene to recent deformation in the thick-skinned fold-and-thrust belt of northwestern Argentina. Tectonics 40, e2020TC006394. https://doi.org/10.1029/2020TC006394.

Flemings, B., Jordan, T.E., 1989. A synthetic stratigraphic model of foreland basin development. J. Geophys. Res. Solid Earth 94, 3851–3866. https://doi.org/10.1029/JB094iB04p03851.

Foster, D.A., Gleadow, A.J.W., 1996. Structural framework and denudation history of the flanks of the Kenya and Anza Rifts, East Africa. Tectonics 15, 258–271. https://doi.org/10.1029/95TC02744.

Garcia Bautista, D.F., dos Santos, Vaz, Neto, E., Penteado, H.L.D.B., 2015. Controls on petroleum composition in the Llanos basin, Colombia: Implications for exploration. AAPG Bull. 99, 1503–1535. https://doi.org/10.1306/03241514152.

Garcia, V.H., Hongn, F., Yagupsky, D., Pingel, H., Kinnaird, T., Winocur, D., 2019. Late Quaternary tectonics controlled by fault reactivation. J. Struct. Geol. 128, 103875. https://doi.org/10.1016/j.jsg.2019.103875.

Grier, M.E., Salfity, J.A., Allmendinger, R.W., 1991. Andean reactivation of the Cretaceous Salta rift, northwestern Argentina. J. South Am. Earth Sci. 4, 351–372. https://doi.org/10.1016/0895-9811(91)90013-X.

Grujic, D., Coutand, I., Bookhagen, B., Bonnet, S., Blythe, A., Duncan, C., 2006. Climatic forcing of erosion, landscape, and tectonics in the Bhutan Himalayas. Geology 34, 801–804. https://doi.org/10.1130/G22806.1.

Gupta, S., Allen, P.A., 2000. Implications of foreland paleotopography for stratigraphic development in the Eocene distal Alpine foreland basin. Geol. Soc. Am. Bull. 112, 515–530. https://doi.org/10.1130/0016-7606(2000)112<515:IOFPTF>2.3.CO;2.
Hain, M.P., Strecker, M.R., Bookhagen, B., Alonso, R.N., Pingel, H., Schmitt, A.K., 2011. Neogene to Quaternary broken foreland formation and sedimentation dynamics in the Andes of NW Argentina (25 S). Tectonics 30, TC2006. https://doi.org/10.1029/2010TC002778.
Heredia, N., García-Sansegundo, J., Farias Arquer, P.J., Alonso Alonso, J.L., Gallastegui Suárez, J., Méndez Bedia, M.I., Rubio Ordóñez, Á., 2016. Evolución Geodinámica de los Andes argentinochilenos y la Península Antártica durante el Neoproterozoico tardío y el Paleozoico. Trab. Geol. 36.
Heredia, N., García-Sansegundo, J., Gallastegui, G., Farias, P., Giacosa, R., Hongn, F., Ramos, V.A., 2018. The pre-andean phases of construction of the southern Andes basement in neoproterozoic-paleozoic times. In: Folguera, A., et al. (Eds.), The Evolution of the Chilean-Argentinean Andes. Springer, Cham, pp. 111–131. https://doi.org/10.1007/978-3-319-67774-3_6.
Hilley, G.E., Blisniuk, P.M., Strecker, M.R., 2005. Mechanics and erosion of basement-cored uplift provinces. J. Geophys. Res. 110, B12409. https://doi.org/10.1029/2005JB003704.
Horton, B.K., 2018. Tectonic regimes of the central and southern Andes: responses to variations in plate coupling during subduction. Tectonics 37, 402–429. https://doi.org/10.1029/2017TC004889.
Horton, B.K., DeCelles, P.G., 1997. The modern foreland basin system adjacent to the Central Andes. Geology 25, 895–898. https://doi.org/10.1130/0091-7613(1997)025<0895:TMFBSA>2.3.CO;2.
Horton, B.K., Folguera, A. (Eds.), 2019. Andean Tectonics. Elsevier, Amsterdam. https://doi.org/10.1016/C2017-0-04053-3.
Howell, J.A., Schwarz, E., Spalletti, L.A., Veiga, G.D., 2005. The Neuquén basin: an overview. Geol. Soc. Lond. Spec. Publ. 252, 1–14. https://doi.org/10.1144/GSL.SP.2005.252.01.01.
Iaffa, D.N., Sábat, F., Muñoz, J.A., Mon, R., Gutierrez, A.A., 2011. The role of inherited structures in a foreland basin evolution. The Metán Basin in Northwest Argentina. J. Struct. Geol. 33, 1816–1828. https://doi.org/10.1016/j.jsg.2011.08.006.
Iaffa, D.N., Sábat, F., Muñoz, J.A., Carrera, N., 2013. Basin fragmentation controlled by tectonic inversion and basement uplift in Sierras Pampeanas and Santa Bárbara System, Northwest Argentina. In: VIII Congreso de Exploración y Desarrollo de Hidrocarburos. IAPG, pp. 1–15 unpublished results.
Jordan, T.E., Isacks, B.L., Allmendinger, R.W., Brewer, J.A., Ramos, V.A., Ando, C.J., 1983. Andean tectonics related to geometry of subducted Nazca plate. Geol. Soc. Am. Bull. 94, 341–361. https://doi.org/10.1130/0016-7606(1983)94<341:ATRTGO>2.0.CO;2.
Kley, J., Monaldi, C.R., 2002. Tectonic inversion in the Santa Barbara System of the central Andean foreland thrust belt, northwestern Argentina. Tectonics 21, 1061. https://doi.org/10.1029/2002TC902003.
Kley, J., Rossello, E.A., Monaldi, C.R., Habighorst, B., 2005. Seismic and field evidence for selective inversion of Cretaceous normal faults, Salta rift, Northwest Argentina. Tectonophysics 399, 155–172. https://doi.org/10.1016/j.tecto.2004.12.020.
Lacombe, O., Bellahsen, N., 2016. Thick-skinned tectonics and basement-involved fold–thrust belts: insights from selected Cenozoic orogens. Geol. Mag. 153, 763–810. https://doi.org/10.1144/GM.2015-055.
Lash, G.G., Engelder, T., 2007. Jointing within the outer arc of a forebulge at the onset of the Alleghanian Orogeny. J. Struct. Geol. 29, 774–786. https://doi.org/10.1016/j.jsg.2007.01.002.
Limarino, C.O., Heredia, N., Spalletti, L.A., Busquets, P., Colombo, F., Méndez-Bedia, I., Césari, S.N., 2023. Stratigraphy and tectosedimentary evolution of the late Paleozoic Ancestral Andes between 33° and 25° SL. J. South Am. Earth Sci. 121, 104116. https://doi.org/10.1016/j.jsames.2022.104116.
Mann, P., Escalona, A., Castillo, M.V., 2006. Regional geologic and tectonic setting of the Maracaibo supergiant basin, western Venezuela. AAPG Bull. 90, 445–477. https://doi.org/10.1306/12020505103.
Marquillas, R.A., Del Papa, C., Sabino, I.F., 2005. Sedimentary aspects and paleoenvironmental evolution of a rift basin: Salta Group (Cretaceous–Paleogene), northwestern Argentina. Int. J. Earth Sci. 94, 94–113. https://doi.org/10.1007/s00531-004-0466-2.
McGlue, M.M., Smith, P.H., Zani, H., Silva, A., Carrapa, B., Cohen, A.S., Pepper, M.B., 2016. An integrated sedimentary systems analysis of the Río Bermejo (Argentina): Megafan character in the overfilled Southern Chaco Foreland basin. Journal of Sedimentary Research 86 (12), 1359–1377. https://doi.org/10.2110/jsr.2016.82.
Meeßen, C., Sippel, J., Scheck-Wenderoth, M., Heine, C., Strecker, M.R., 2018. Crustal structure of the Andean foreland in Northern Argentina. J. Geophys. Res. Solid Earth 123, 1875–1903. https://doi.org/10.1002/2017JB014902.
Molnar, P., England, P., Martinod, J., 1993. Constraints on the uplift and faulting of the Tibetan Plateau from an analysis of buoyancy forces. J. Geophys. Res. Solid Earth 98, 11767–11782. https://doi.org/10.1029/93JB00835.
Moreno, J.A., 1973. Stratigraphy Report of the Well YPF.SE.LH.x-2 (Santiago del Estero, Argentina). YPF S.A., unpublished results).
Mutti, M., Vallati, M., Tomás, S., Galli, C., Rumbelsperger, A.M.B., Maerz, S., Coira, B., 2023. Constraining depositional evolution and reservoir compartmentalization in a mixed carbonate-siliciclastic lacustrine system: the Yacoraite formation, Salta Group, NW Argentina. Mar. Pet. Geol. 149, 106049. https://doi.org/10.1016/j.marpetgeo.2023.106049.
Obermeier, P., Duschl, F., Drews, M.C., 2025. Lithologically constrained velocity–density relationships and vertical stress gradients in the North Alpine Foreland Basin, SE Germany. Solid Earth 16, 425–440. https://doi.org/10.5194/se-16-425-2025.
Oncken, O., Hindle, D., Kley, J., Elger, K., Victor, P., Schemmann, K., 2006. Deformation of the central Andean upper plate system. In: Oncken, O., et al. (Eds.), The Andes: Active Subduction Orogeny. Springer, Berlin, pp. 3–27. https://doi.org/10.1007/978-3-540-48281-2_1.
Peacock, D.C., Banks, G.J., 2020. Basement highs: Definitions, characterisation and origins. Basin Res. 32, 1685–1710. https://doi.org/10.1111/bre.12450.
Pluspetrol, S.A., 1990. Stratigraphy Report of the Well Pluspetrol.SE.Ch-x1001 (Santiago del Estero, Argentina). Pluspetrol S.A., unpublished results.
Ramos, V.A., 1999. Rasgos estructurales del territorio argentino. In: Caminos, R. (Ed.), Geología Argentina, Anales, 29. Subsecretaría de Minería de la Nación, Buenos Aires, pp. 15–75.
Ramos, V.A., Alonso, R.N., 1995. El Mar Paranense en la provincia de Jujuy. Rev. Inst. Geol. Miner. 10, 73–80.
Ramos, V.A., Alonso, R.N., Strecker, M., 2006. Estructura y neotectónica de Las Lomas de Olmedo, zona de transición entre los Sistemas Subandino y de Santa Bárbara, provincia de Salta. Rev. Asoc. Geol. Argent. 61, 579–588. https://doi.org/10.46746/raga.2006.v61.i4.579.
Rapela, C.W., Pankhurst, R.J., Casquet, C., Fanning, C.M., Baldo, E.G., González-Casado, J.M., Galindo, C., Dahlquist, J., 2007. The Río de la Plata craton and the assembly of SW Gondwana. Earth Sci. Rev. 83, 49–82. https://doi.org/10.1016/j.earscirev.2007.03.005.
Reinante, S., Olivieri, G., Salinas, A., Lovecchio, J.P., Basile, Y., 2014. La cuenca Chacoparaná: estratigrafía y recursos de hidrocarburos. In: XIX Congreso Geológico Argentino, Córdoba, pp. 895–912.
Reis, H.L., Suss, J.F., Fonseca, R.C., Alkmim, F.F., 2017. Ediacaran forebulge grabens of the southern São Francisco basin, SE Brazil. Precambrian Res. 302, 150–170. https://doi.org/10.1016/j.precamres.2017.08.016.
Repasch, M., Scheingross, J.S., Hovius, N., Lupker, M., Wittmann, H., Haghipour, N., Gröcke, D.R., Orfeo, O., Eglinton, T.I., Sachse, D., 2021. Fluvial organic carbon cycling regulated by sediment transit time and mineral protection. Nat. Geosci. 14, 842–848. https://doi.org/10.1038/s41561-021-00827-0.
Repasch, M., Scheingross, J.S., Cook, K.L., Sachse, D., Dosch, S., Orfeo, O., Hovius, N., 2023. Lithospheric flexure controls on geomorphology, hydrology, and river chemistry in the Andean foreland basin. AGU Adv. 4, e2023AV000924. https://doi.org/10.1029/2023AV000924.
Reyes, F.C., Salfity, J.A., 1973. Consideraciones sobre la estratigrafía del Cretácico (Subgrupo Pirgua) del noroeste argentino. In: V Congreso Geológico Argentino. Asociación Geológica Argentina, Actas III, Buenos Aires, pp. 355–385.
Roddaz, M., Baby, P., Brusset, S., Hermoza, W., Darrozes, J.M., 2005. Forebulge dynamics and environmental control in Western Amazonia: the case study of the Arch of Iquitos (Peru). Tectonophysics 399, 87–108. https://doi.org/10.1016/j.tecto.2005.01.009.
Rolleri, E.O., 1965. Stratigraphy Report of the Well YPF.F-P-1 (Formosa, Argentina). YPF S.A., unpublished results.
Rolleri, E.O., 1966. Stratigraphy Report of the Well YPF.CHA.LBO-x1 (Chaco, Argentina). YPF S.A., unpublished results.
Rolleri, E.O., 1967. Stratigraphy Report of the Well YPF.CHA.LB-x2 (Chaco, Argentina). YPF S.A., unpublished results.
Ruiz-Monroy, R., 2021. Organic Geochemical Characterization of the Yacoraite Formation (NW-Argentina)-Paleoenvironment and Petroleum Potential. Doctoral dissertation,. Universität Potsdam.
Russo, A., Ferello, R.E., Chebli, G., 1979. Cuenca Chacopampena. In: Turner, J.C.M. (Ed.), Geología Regional Argentina, vol. 1. Academia Nacional de Ciencias, Córdoba, pp. 139–183.
Salfity, J.A., Marquillas, R.A., 1994. Tectonic and sedimentary evolution of the Cretaceous-Eocene Salta Group Basin, Argentina. In: Salfity, J.A. (Ed.), Cretaceous Tectonics of the Andes. Vieweg, Braunschweig, pp. 266–315. https://doi.org/10.1007/978-3-663-12004-7_11.
Sarmiento, L.F., Rangel, A., 2004. Petroleum systems of the upper Magdalena Valley, Colombia. Mar. Pet. Geol. 21, 373–391. https://doi.org/10.1016/j.marpetgeo.2003.11.006.
Sinclair, H.D., Coakley, B.J., Allen, P.A., Watts, A.B., 1991. Simulation of foreland basin stratigraphy using a diffusion model of mountain belt uplift and erosion: an example from the Central Alps, Switzerland. Tectonics 10, 599–620. https://doi.org/10.1029/90TC02720.
Spickert, A., 2014. Petroleum System Analysis: Middle Magdalena Valley Basin, Colombia, South America. M.S. thesis. University of Washington.
Starck, D., 2011. Cuenca Cretácica-Paleógena del noroeste argentino. In: VIII Congreso de Exploración y Desarrollo de Hidrocarburos. IAPG, Buenos Aires, pp. 407–453.
Stauffer, K.W., Croft, G.D., 1995. A modern look at the petroleum geology of the Maracaibo basin, Venezuela. Oil Gas J. 93.
Strecker, M.R., Hilley, G.E., Bookhagen, B., Sobel, E.R., 2011. Structural, geomorphic, and depositional characteristics of contiguous and broken foreland basins. In: Busby, C., Pérez, A.A. (Eds.), Tectonics of Sedimentary Basins: Recent Advances. Wiley-Blackwell, Chichester, pp. 508–521. https://doi.org/10.1002/9781444347494.ch24.
Torre, G., Coppo, R., Jara, D.M., Nogués, V., Cosentino, N.J., Tur, V., Gilli, S., Gaiero, D. M., 2025. Late Pleistocene-Holocene Dust Record in the Pampa Plain. In: Perez, S.I., et al. (Eds.), Pampean Lakes. Springer, Cham, pp. 25–50. https://doi.org/10.1007/978-3-031-64551-5_3.
Torres Acosta, V., Bande, A., Sobel, E.R., Parra, M., Schildgen, T.F., Stuart, F., Strecker, M.R., 2015. Cenozoic extension in the Kenya Rift from low-temperature thermochronology: Links to diachronous spatiotemporal evolution of rifting in East Africa. Tectonics 34, 2367–2386. https://doi.org/10.1002/2015TC003949.
Trice, R., 2014. Basement Exploration, West of Shetlands: Progress in Opening a New Play on the UKCS. Geol. Soc. Lond, London.
Turcotte, D., Schubert, G., 2014. Geodynamics, third ed. Cambridge University Press, Cambridge.

Turner, J.C.M., 1959. Estratigrafía del cordón de Escaya y de la sierra de Rinconada (Jujuy). Rev. Asoc. Geol. Argent. 13, 15–41.

Vallati, M., Tomás, S., Galli, C., Winterleitner, G., Mutti, M., 2023. Depositional controls in an ancient, closed lake system: a high-resolution and multi-scalar case study from the Yacoraite Formation (Salta Basin, Argentina). Sediment. Geol. 450, 106456. https://doi.org/10.1016/j.sedgeo.2023.106456.

Veiga, R.D., Vergani, G.D., Brissón, I.E., Macellari, C.E., Leanza, H.A., 2020. The Neuquén super basin. AAPG Bull. 104, 2521–2555. https://doi.org/10.1306/07132020101.

Watts, A.B., 2001. Isostasy and Flexure of the Lithosphere. Cambridge University Press, Cambridge.

White, T., Furlong, K., Arthur, M., 2002. Forebulge migration in the Cretaceous Western Interior basin of the Central United States. Basin Res. 14, 43–54. https://doi.org/10.1046/j.1365-2117.2002.00168.x.

Zapata, S., Sobel, E.R., Del Papa, C., Glodny, J., 2020. Upper plate controls on the formation of broken foreland basins in the Andean retroarc between 26 S and 28 S: from Cretaceous rifting to Paleogene and Miocene broken foreland basins. Geochem. Geophys. Geosyst. 21, e2019GC008876. https://doi.org/10.1029/2019GC008876.